Geophys. J. Int. (1997) **131**, 699–723

Some remarks about the degree-one deformation of the Earth

Marianne Greff-Lefftz* and Hilaire Legros

Institut de Physique du Globe de Strasbourg, 5 rue R. Descartes 67084, *Strasbourg, France. E-mail: greff@ipgp.jussieu.fr*

Accepted 1997 July 1. Received 1997 March 3; in original form 1996 February 23

SUMMARY

The degree-one deformation of the Earth (and the induced discrepancy between the figure centre and the mass centre of the Earth) is computed using a theoretical approach (Love numbers formalism) at short timescales (where the Earth has an elastic behaviour) as well as at long timescales (where the Earth has a viscoelastic or quasi-fluid behaviour). For a Maxwell model of rheology, the degree-one relaxation modes associated with the viscoelastic Love numbers have been investigated: the M_o mode does not exist and there is only one transition mode (instead of two) generated by a viscosity discontinuity.

The translations at each interface of the incompressible layers of the earth model [surface, 670 km depth discontinuity, core–mantle boundary (CMB) and inner-core boundary (ICB)] are computed. They are elastic with an order of magnitude of about 1 mm when the excitation source is the atmospheric continental loading or a magnetic pressure acting at the CMB. They are viscoelastic when the earth is submitted to Pleistocene deglaciation, with an order of magnitude of about 1 m. In a quasi-fluid approximation (Newtonian fluid) because of the mantle density heterogeneity their order of magnitude is about 100 m (except for the ICB, which is in quasi-hydrostatic equilibrium at this timescale).

Key words: deformation, elasticity, relaxation modes, viscoelasticity.

1 INTRODUCTION

Degree-one deformation has particular characteristics related to geodesy as well as to mechanics: it is related to the centre of mass of the Earth and is strongly dependent on the choice of the origin of the reference frame.

We have first to provide some precise definitions concerning these reference frames. We consider an initial undeformed reference sphere that is radially stratified. The geometric centre of the external spherical surface is coincident with that of each layer, and is identical to the centre of mass of the whole sphere. For a degree-one deformation, the external surface of the planet remains spherical but is translated with respect to the initial configuration; similarly, each internal layer of the planet is translated but the centre of mass does not change and remains fixed relative to the centre of the initial reference sphere. We define the figure centre as the geometric centre of the translated external spherical surface. The geometric centres of the various internal layers move in the deformed configuration and are different to the figure centre; they do not play any geodetic role and will not be given precisely (but they may be easily computed).

The sources of degree-one deformation are essentially internal or external redistributed loads (including the atmosphere and the oceans), that is without net change in the total mass of the Earth. With respect to the reference configuration, a load is the expression of a mass transfer from a given hemisphere to the other one. This is observed for atmospheric and oceanic loading. For solid-mass anomalies, such as ice sheets, cool internal zones, surface tectonics, etc., the conservation of the centre of mass imposes a displacement of the particles in a direction opposite to that of the mass anomalies. This displacement is distributed within the whole planet.

* Now at: Institut de Pysique du Globe de Paris, Département de Géomagnetisme, 4 place Jussieu, 75252 Paris 05, France.

Degree-one deformation involving a translation of the external surface may have some geodetic consequences. In fact, observation stations, being located on the external surface, undergo the surface translation. If these stations are used to define a reference frame, the centre of this frame will be the figure centre of the translated Earth and will not be the centre of mass. This discrepancy between the centre of figure and the centre of mass may be taken into account in the observations of satellites, whose trajectories are related to the centre of mass. Note that, in addition to this surface translation, the stations also undergo tangential displacements (for degree one as well as for the other degrees), which create perturbations, especially in the angular measurements. On the other hand, note that, contrary to the solid surface, which is translated, the oceans, whose form is related to the equipotential, do not move (in the absence of atmospheric perturbation), because the conservation of the centre of mass means that there is no perturbation in the surface potential, that is in the degree-one geoid. The observation of variations in sea level could be a simple test to detect degree-one deformation.

Another type of degree-one deformation is the degree-one tidal potential due to the terrestrial bulge acting on the Moon (Wilhelm 1983; Dahlen 1993). This source is very different from the loading excitation. In fact, the reference frame related to the Earth's centre of mass moves with respect to the centre of mass of the Earth–Moon system. The resulting acceleration could be detected with gravimeters, for example, but it is a rigid translation and there is no relative displacement within the Earth.

In this paper, we work in a frame related to the Earth with an origin at the centre of mass itself and we assume that the sources of deformation do not create a net change in the total mass of the Earth. In this frame, the total degree-one force acting has to be equal to zero (Okubo & Endo 1986); this is the case for a surface load, for example, where the effect in potential is compensated by the pressure effect, such that the total degree-one resulting force is zero (e.g. Farrell 1972; Cathles 1975). A degree-one redistributed surface load (that is without net changes in the total mass) will involve degree-one displacements at the surface and within the whole planet, and in particular a discrepancy between the centre of figure and the conserved centre of mass.

The aim of this paper is to investigate these deformations at different timescales.

(1) At short timescales, the behaviour of the Earth is elastic. Atmospheric and oceanic loading are observed (with periods of less than two years), with a degree-one coefficient in the spherical-harmonic expansion (Gegout 1995), due both to the distribution of the oceans at the Earth's surface (most of the continents are in the Northern hemisphere) and to the motions within the atmosphere. A spherical-harmonic analysis of the pressure field variation shows the existence of the degree-one loading term (Gegout 1995), which may be considered as a transfer of atmospheric masses from a given hemisphere to the other one: this transfer is compensated by a translation of the Earth (in the opposite direction) in order to conserve the centre of mass.

(2) At decade timescales, magnetic pressures (Hulot 1992) as well as viscous tractions exist at the core–mantle boundary (CMB) and at the inner-core–outer-core boundary (ICB), induced by the fluid motions. These internal pressures and tangential tractions involve degree-one elastic deformation.

(3) At longer timescales, the melting of the Canadian, Fennoscandian and Antartic ice sheets produces surface loads containing degree-one terms (e.g. Peltier & Wu 1983). Taking into account the viscoelastic response of the Earth (Peltier 1974; Wu & Peltier 1982), this deglaciation involves present degree-one deformation within the Earth (Wu 1990).

(4) At geological timescales, internal loading is induced by density anomalies and deforms the Earth (Hager 1984; Richards & Hager 1984; Hager *et al.* 1985; Forte, Dziewonski & Woodward 1993; Greff-Lefftz & Legros 1996). There is a shift of the surface with respect to the hydrostatic equipotential (that is a shift of the figure centre with respect to the mass centre), which will be computed.

The equations governing the elastic deformation within a pre-stress planet are the impulsion equation, the conservation of mass and the Poisson equation. A rheological law is necessary to relate the stress to the strain. In the classical elastogravitational theory, the displacement vector field and the traction are expanded in spherical spheroidal vectors of degree n and order m. For $n \geq 1$, the equations may be written as sixth-order differential equations in the form given by Alterman, Jarosch & Pekeris (1959). For the degree $n = 1$, there are two problems: the classical boundary conditions are not independent and the centre of mass of the Earth is not conserved. In this paper, we propose a theoretical approach using a Love number formalism for the degree-one deformations, starting from the classical elastogravitational set of equations and taking into account the conservation of the centre of mass (Farrell 1972). Our earth model is incompressible and consists of an elastic lithosphere, a stratified mantle, an inviscid homogeneous fluid core and a homogeneous inner core. The deformation is investigated at each interface of the model (surface, 670 km depth discontinuity, CMB and ICB).

In the first part of this paper, we are interested in the elastic deformation (that is deformation at timescales less than the decade), in particular the nearly annual translation induced by atmospheric continental loading and the decadal deformation due to the geostrophic magnetic pressure acting at the CMB.

In the second part, we assume that the Earth has a Maxwell rheological model. First, the number of relaxation modes associated with the viscoelastic Love numbers is studied, and then some geophysical applications are investigated, such as the translations induced by the Pleistocene deglaciation, and at longer timescales, in a quasi-fluid approximation, the degree-one deformation resulting from the mantle-density heterogeneity.

2 ELASTIC THEORY

2.1 Equations

2.1.1 Analytical solutions

The classical elastogravitational theory is a theory of perturbation. We start with an initial state where the earth is assumed to be in hydrostatic equilibrium, radially stratified following the PREM model (Dziewonski & Anderson 1981). The origin of the reference frame is the centre of mass, which is identical to the centre of geometry of the sphere at this initial state. In the perturbed state, the earth is elastic and the equations are always written in a reference frame related to the centre of mass.

The differential equations governing the spheroidal part of the displacement field, the stresses and the body-force potentials are of sixth order. Expanding the displacement vector field $\mathbf{u}$ and the traction $\mathbf{T}$ in spherical spheroidal vectors, ∇_H denoting the tangential gradient, we obtain the following:

$$\mathbf{u}=\sum_{n=1}^{\infty}\sum_{m=0}^{n} y_{1n}(r)\,Y_n^m(\theta,\varphi)\frac{\mathbf{r}}{r}+ry_{3n}(r)\nabla_H Y_n^m(\theta,\varphi), \tag{1}$$

$$\mathbf{T}=\sum_{n=1}^{\infty}\sum_{m=0}^{n} y_{2n}(r)\,Y_n^m(\theta,\varphi)\frac{\mathbf{r}}{r}+ry_{4n}(r)\nabla_H Y_n^m(\theta,\varphi), \tag{2}$$

where the potential

$$U=\sum_{n=1}^{\infty}\sum_{m=0}^{n} y_{5n}(r)\,Y_n^m(\theta,\varphi),$$

and introducing a function defined by

$$y_{6n}(r)=\frac{dy_{5n}(r)}{dr}-4\pi G\rho y_{1n}(r) \tag{3}$$

for the radial derivative of the potential, where Y_n^m are the spherical harmonics, θ the colatitude and φ the longitude, the system can be written

$$\frac{dy_i(r)}{dr}=A_{ij}\,y_j(r) \tag{4}$$

(Alterman *et al.* 1959), where A_{ij} is a 6×6 matrix whose elements are a function of the compressibility $\lambda(r)$, the rigidity $\mu(r)$, the density $\rho(r)$ and the gravity $g(r)$.

Our earth model consists of N homogeneous layers (Fig. 1): an elastic lithosphere (layer 1), a stratified elastic mantle (layers 2 to $N-2$), an inviscid fluid core (layer $N-1$) and an elastic inner core (layer N). The planet is assumed to be incompressible. In each homogeneous elastic layer i (that is in each layer except the fluid core) with a density ρ^i and a constant rigidity μ^i, solving the system (4) the $y_{in}(r)$ may be written as follows:

$$\begin{pmatrix} y_{1n}^i(r)\\ y_{2n}^i(r)\\ y_{3n}^i(r)\\ y_{4n}^i(r)\\ y_{5n}^i(r)\\ y_{6n}^i(r)\end{pmatrix}=\begin{pmatrix} \frac{1}{r^n} & \frac{1}{r^{(n+2)}} & r^{n+1} & r^{n-1} & 0 & 0\\ \frac{-2\mu^i\frac{n^2+3n-1}{n+1}+\rho^i gr}{r^{(n+1)}} & \frac{-2\mu^i(n+2)+\rho^i gr}{r^{(n+3)}} & \frac{2\mu^i\frac{n^2-n-3}{n}+\rho^i gr}{r^{-n}} & \frac{2\mu^i(n-1)+\rho^i gr}{r^{(2-n)}} & -\rho^i r^n & -\frac{\rho^i}{r^{(n+1)}}\\ \frac{2-n}{n(n+1)}\frac{1}{r^n} & -\frac{1}{n+1}\frac{1}{r^{(n+2)}} & \frac{n+3}{n(n+1)}r^{n+1} & \frac{1}{n}r^{n-1} & 0 & 0\\ \frac{n-1}{n}\frac{2\mu^i}{r^{(n+1)}} & \frac{n+2}{n+1}\frac{2\mu^i}{r^{(n+3)}} & \frac{n+2}{n+1}2\mu^i r^n & \frac{n-1}{n}2\mu^i r^{n-2} & 0 & 0\\ 0 & 0 & 0 & 0 & r^n & \frac{1}{r^{(n+1)}}\\ \frac{-4\pi G\rho^i}{r^n} & \frac{-4\pi G\rho^i}{r^{(n+2)}} & -4\pi G\rho^i r^{n+1} & -4\pi G\rho^i r^{n-1} & nr^{n-1} & -\frac{(n+1)}{r^{(n+2)}}\end{pmatrix}\begin{pmatrix} C_{1n}^i\\ C_{2n}^i\\ C_{3n}^i\\ C_{4n}^i\\ C_{5n}^i\\ C_{6n}^i\end{pmatrix} \tag{5}$$

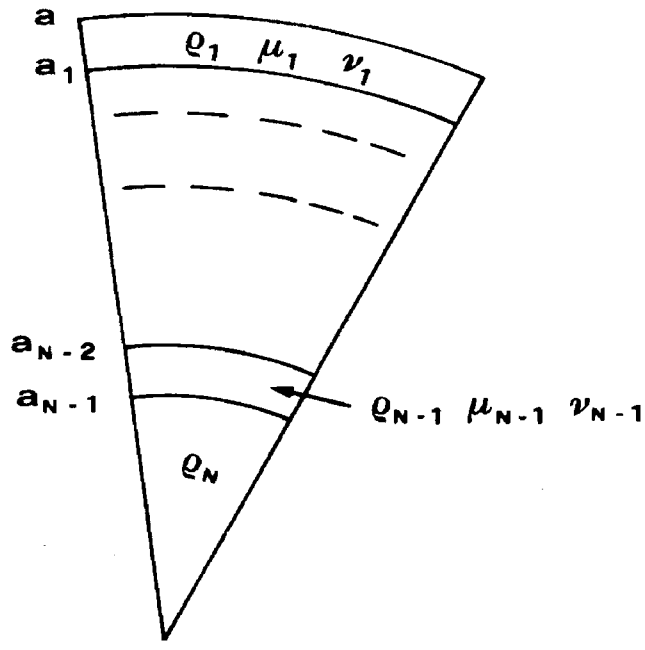

Figure 1. Earth model consisting of N incompressible homogeneous layers: an elastic lithosphere, $N-3$ viscoelastic layers describing the mantle, an inviscid fluid core and a viscoelastic inner core. Earth layer i is defined by a radius a_i in metres, with a the radius of the earth's surface, $b=a_{N-2}$ the core radius and $c=a_{N-1}$ the inner-core radius, a density ρ_i in kg m^{-3} and an elastic rigidity μ_i in Pa.

(e.g. Wu & Peltier 1982; Spada *et al.* 1990), where G is the gravitational constant and C^i_{1n}, C^i_{2n}, C^i_{3n}, C^i_{4n}, C^i_{5n} and C^i_{6n} for $i=1, \ldots, N-2, N$ are $6\times(N-1)$ unknown constants which will be determined by the boundary conditions.

Within the inviscid fluid core, the system (4) is not valid. The equations of motion reduce to a set of two ordinary differential equations in y_5^{N-1} and y_6^{N-1} (Smylie & Mansinha 1971):

$$\frac{dy_i^{N-1}(r)}{dr} = B_{ij}\, y_j(r) \qquad \text{for} \quad i=5,6\,, \tag{6}$$

where B_{ij} is a 2×2 matrix whose elements are a function of the density $\rho(r)$ and the gravity $g(r)$.

The boundary conditions have been discussed by Chinnery (1975), Crossley & Gubbins (1975) and Dahlen & Fels (1978). In this paper, we use the theoretical approach introduced by Chinnery (1975):

(1) the radial stress is equal to zero: $y_2^{N-1}(r)=0$;
(2) the tangential displacement $y_3^{N-1}(r)$ is undetermined;
(3) the form is the equipotential; we may define a radial displacement $y_1^{N-1}(r)$ as the high of the equipotential:

$$y_1^{N-1}(r)=\frac{y_5^{N-1}(r)}{g(r)}\,.$$

The solutions for a homogeneous incompressible fluid core may be written

$$\begin{cases} y_{5n}^{N-1}(r)=C_{5n}^{N-1}r^n+\dfrac{C_{6n}^{N-1}}{r^{n+1}} \\ y_{6n}^{N-1}(r)=nC_{5n}^{N-1}r^{n-1}-(n+1)\dfrac{C_{6n}^{N-1}}{r^{n+2}}-4\pi G\rho^{N-1}y_{1n}^{N-1}(r) \end{cases}, \tag{7}$$

where C_{5n}^{N-1} and C_{6n}^{N-1} are two unknown constants.

2.1.2 Excitation sources

Knowing the propagators within the earth, we have to write the boundary conditions between each layer of our earth model in order to determine the unknown constants. In this paper we are particularly interested in the effect of internal loads on the degree-one deformation. A degree-n superficial mass distribution $\sigma(r_o)$, located at the radius r_o within the mantle, produces two effects:

(1) a degree-n pressure effect, $-g(r_o)\sigma(r_o)$, acting at the radius $r=r_o$;

(2) a degree-n potential effect,

$$V^{in}=\frac{4\pi G}{2n+1}\sigma(r_o)r_o\begin{cases}\left(\frac{r}{r_o}\right)^n & \text{if } r\le r_o\\ \left(\frac{r_o}{r}\right)^{n+1} & \text{if } r\ge r_o\end{cases}.$$

Surface pressure, P^e (a dynamical pressure related to motion within the atmosphere, for example), and internal pressures (with a magnetic origin), P^c and P^{ic}, within the core, acting respectively at the CMB and the ICB, and a surface load, S^e, will also be taken into account. T^e, T^c and T^{ic} denote tangential tractions acting respectively at the surface (induced by friction on the mountains or at the bottom of the oceans), at the CMB and at the ICB (viscous friction). These internal tangential tractions do not exist if the core is assumed to be inviscid, but may exist in a weak boundary layer at the CMB or at the ICB.

2.1.3 *Boundary conditions*

When the earth is submitted to these different excitation sources, the boundary conditions may be written as follows.

(1) At the surface $r=a$: the tangential stress is equal to the acting tangential traction and the radial stress to the acting pressure; the discontinuity in the gravity leads to a relation between $y_6^1(a)$, $y_5^1(a)$ and the acting potential,

$$\begin{cases}y_4^1(a)=T^e\\ y_2^1(a)=-P^e-\dfrac{2n+1}{3}\tilde{\rho}S^e\\ y_6^1(a)+\dfrac{n+1}{a}y_5^1(a)=\dfrac{2n+1}{a}S^e\end{cases}, \tag{8}$$

where $\tilde{\rho}$ is the mean density of the earth.

(2) At an interface a_i within the mantle: the radial and tangential displacements, the tangential stress and the potential are continuous; taking into account an internal-loading potential V^{in} acting at the radius r_o the continuity of the radial stress and that for the gravity at an interface a_i will depend on this excitation source if $a_i=r_o$,

$$\begin{cases}y_1^i(a_i)=y_1^{i+1}(a_i);\quad y_3^i(a_i)=y_3^{i+1}(a_i);\quad y_4^i(a_i)=y_4^{i+1}(a_i);\quad y_5^i(a_i)=y_5^{i+1}(a_i)\\ y_2^i(a_i)-y_2^{i+1}(a_i)=\dfrac{2n+1}{3}\dfrac{g(a_i)}{g_o}\dfrac{a}{a_i}\tilde{\rho}V^{in}\delta(a_i-r_o)\\ y_6^i(a_i)-y_6^{i+1}(a_i)=-(2n+1)\dfrac{V^{in}}{a_i}\delta(a_i-r_o)\end{cases}, \tag{9}$$

where $\delta(a_i-r_o)$ is the Dirac function, which is equal to 1 if $a_i=r_o$, the radius where the load is located, and to 0 if $a_i\neq r_o$, and g_o is the surface gravity.

(3) At the CMB: the radial displacement is continuous but we have to introduce an unknown parameter K_1 in order to take into account the difference between the form of the solid mantle and the form of the fluid core, which is an equipotential (Chinnery 1975); the tangential displacement is not determined; the tangential stress is equal to the acting tangential traction (the negative sign comes from the fact that the tangential traction is expressed following the outer normal of the mantle at the CMB); the gravitational potential is continuous; the continuity of the radial stress depends on the fluid pressure acting within the core; the gravity of the mantle is related to that of the fluid core, taking into account the discrepancy K_1:

$$\begin{cases}y_1^{N-2}(a_{N-2})=y_1^{N-1}(a_{N-2})+a_{N-2}K_1\\ y_3^{N-2}(a_{N-2})=a_{N-2}K_3\\ y_4^{N-2}(a_{N-2})=-T^c\\ y_5^{N-2}(a_{N-2})=y_5^{N-1}(a_{N-2})\\ y_2^{N-2}(a_{N-2})=\rho^{N-1}g(a_{N-2})a_{N-2}K_1-P^c\\ y_6^{N-2}(a_{N-2})=y_6^{N-1}(a_{N-2})-4\pi G\rho^{N-1}a_{N-2}K_1\end{cases}. \tag{10}$$

(4) At the ICB: the radial displacement is continuous but we have to introduce an unknown parameter K_2 in order to take into account the difference between the form of the solid inner core and the form of the fluid core, which is an equipotential; the tangential displacement is not determined; the tangential stress is equal to the acting tangential traction at the ICB; the gravitational potential is continuous; the continuity of the radial stress depends on fluid pressure within the core acting at the ICB; and the gravity of the

inner core is related to that of the fluid core, taking into account the discrepancy K_2:

$$\begin{cases} y_1^{N-1}(a_{N-1}) - a_{N-1}\,K_2 = y_1^N(a_{N-1}) \\ y_3^N(a_{N-1}) = a_{N-1}\,K_4 \\ y_4^N(a_{N-1}) = T^{ic} \\ y_5^{N-1}(a_{N-1}) = y_5^N(a_{N-1}) \\ -\rho^{N-1} g(a_{N-1}) a_{N-1} K_2 - P^{ic} = y_2^N(a_{N-1}) \\ y_6^{N-1}(a_{N-1}) + 4\pi G \rho^{N-1} a_{N-1} K_2 = y_6^N(a_{N-1}) \end{cases} \tag{11}$$

Assuming that in the homogeneous inner core the displacement and the potential cannot diverge at the origin $r=0$, we have $C_1^N = C_2^N = C_6^N = 0$. Consequently, in the mantle there are C_1^i, C_2^i, C_3^i, C_4^i, C_5^i, C_6^i, for $i=1, \ldots, N-2$, undetermined constants, in the fluid core there are C_5^{N-1}, C_6^{N-1}, K_1, K_2, K_3, K_4 undetermined constants and in the inner core there are C_3^N, C_4^N, C_5^N undetermined constants, that is $6N-3$ unknowns. The numbers of boundary conditions is three for the surface and $6\times(N-1)$ for the other interfaces, that is $6N-3$ equations. For $n \neq 1$ the determinant of this set of boundary conditions is not equal to zero and the system can be solved; the solutions $y_i(r)$, for $i=1, \ldots, 6$, may then be deduced within the entire earth.

2.1.4 Degree-one case and consistency relation

For the degree $n=1$, there are two problems: first, in the set of $(6N-3)$ equations (8), (9), (10) and (11), only $(6N-4)$ equations are independent, and second, the centre of mass of the earth is not conserved. In fact, the elastic solutions given by the propagator matrix do not automatically meet this requirement. According to the well-known formula of MacCullagh (e.g. Munk & MacDonald 1960), the conservation of the centre of mass will simply require that the degree-one surface potential is equal to zero, that is we just have to add a surface boundary condition,

$$y_5^1(a) = 0\,. \tag{12}$$

We thus obtain a set of $6N-3$ independent equations and the system can be analytically solved. The last equation (the non-independent one) will be automatically verified as a relation between the excitation sources, and in particular will require the global resulting force acting at the solid–fluid interfaces of the earth to be equal to zero,

$$a^2(P^e - 2T^e) + b^2(-P^c - 2T^c) + c^2(P^{ic} - 2T^{ic}) = 0\,, \tag{13}$$

where, for simplicity, $b = a_{N-2}$ is the outer-core radius and $c = a_{N-1}$ is the inner-core radius. This relation has a simple explanation: in order to conserve the centre of mass of the earth, the total force acting on the earth must be equal to zero. Pressures P^e, P^c and P^{ic} and tangential tractions T^e, T^c and T^{ic} involve a force $\mathbf{F}$, such that

$$\mathbf{F} = \int_{\text{surface}} -P^e\,Y_n\mathbf{n} + \boldsymbol{\nabla}_H[T^e\,Y_n]\,ds + \int_{\text{CMB}} P^c\,Y_n\mathbf{n} + \boldsymbol{\nabla}_H[T^c\,Y_n]\,ds + \int_{\text{ICB}} -P^{ic}\,Y_n\mathbf{n} + \boldsymbol{\nabla}_H[T^{ic}\,Y_n]\,ds\,, \tag{14}$$

where $\mathbf{n} = (\sin\theta\cos\varphi,\ \sin\theta\sin\varphi,\ \cos\theta)$ is the outer normal of the solid spherical mantle (θ being the colatitude and φ the longitude) and $Y_n(\theta, \varphi)$ is the degree-n spherical harmonic. This force is equal to zero (because of the orthogonality of the spherical harmonics) except for a degree-one pressure and tangential traction. Noting the following:

$$\begin{aligned} &P^e\,Y_1(\theta,\varphi) = p_1^{0e}\cos\theta + (p_1^{1e}\cos\varphi + \tilde{p}_1^{1e}\sin\varphi)\sin\theta\,, \\ &P^c\,Y_1(\theta,\varphi) = p_1^{0c}\cos\theta + (p_1^{1c}\cos\varphi + \tilde{p}_1^{1c}\sin\varphi)\sin\theta\,, \\ &P^{ic}\,Y_1(\theta,\varphi) = p_1^{0ic}\cos\theta + (p_1^{1ic}\cos\varphi + \tilde{p}_1^{1ic}\sin\varphi)\sin\theta\,, \\ &T^e\,Y_1(\theta,\varphi) = t_1^{0e}\cos\theta + (t_1^{1e}\cos\varphi + \tilde{t}_1^{1e}\sin\varphi)\sin\theta\,, \\ &T^c\,Y_1(\theta,\varphi) = t_1^{0c}\cos\theta + (t_1^{1c}\cos\varphi + \tilde{t}_1^{1c}\sin\varphi)\sin\theta\,, \\ &T^{ic}\,Y_1(\theta,\varphi) = t_1^{0ic}\cos\theta + (t_1^{1ic}\cos\varphi + \tilde{t}_1^{1ic}\sin\varphi)\sin\theta\,, \end{aligned} \tag{15}$$

the resulting force $\mathbf{F}$, in a geographic frame (centred at the centre of mass), is

$$\mathbf{F} = \frac{4}{3}\pi a^2 \begin{pmatrix} -p_1^{1e} + 2t_1^{1e} \\ -\tilde{p}_1^{1e} + 2\tilde{t}_1^{1e} \\ -p_1^{0e} + 2t_1^{0e} \end{pmatrix} + \frac{4}{3}\pi b^2 \begin{pmatrix} p_1^{1c} + 2t_1^{1c} \\ \tilde{p}_1^{1c} + 2\tilde{t}_1^{1c} \\ p_1^{0c} + 2t_1^{0c} \end{pmatrix} + \frac{4}{3}\pi c^2 \begin{pmatrix} -p_1^{1ic} + 2t_1^{1ic} \\ -\tilde{p}_1^{1ic} + 2\tilde{t}_1^{1ic} \\ -p_1^{0ic} + 2t_1^{0ic} \end{pmatrix}, \tag{16}$$

This force must be equal to zero and consequently imposes the following relation on the degree-one coefficients of the pressures and frictions: $a^2(-P^e + 2T^e) + b^2(P^c + 2T^c) + c^2(-P^{ic} + 2T^{ic}) = 0$.

We want to investigate the connection between this equation and the Consistency Relation introduced by Farrell (1972). According to Farrell (1972) (see also Okubo & Endo 1986), only two of the three surface conditions are needed and the Consistency Relation ensures that the third boundary condition is met automatically. This Consistency Relation is a special condition that the degree-one valid solutions have to obey. Farrell (1972) wrote this relation when the earth is submitted to a surface load:

$$y_2(r)+2y_4(r)+\frac{g(r)}{4\pi G}\left[y_6(r)+\frac{2}{r}y_5(r)\right]=0. \tag{17}$$

This has been proved using the reciprocity theorem (Saito 1974) and interpreted by Okubo & Endo (1986) as implying that in the static case there cannot be net force on any portion of the earth.

We wish to rewrite this Consistency Relation when the earth is submitted to external and internal pressures and tangential traction. We start from the y_i system (4) within the elastic parts of the earth, and combining the equations we show that for $n=1$

$$\frac{d}{dr}\left[r^2\left(y_2(r)+2y_4(r)+\frac{g(r)}{4\pi G}\left[y_6(r)+\frac{2}{r}y_5(r)\right]\right)\right]=0. \tag{18}$$

Within the fluid core, the set of two ordinary differential equations (6) will involve the following for $n=1$:

$$\frac{d}{dr}\left[r^2\frac{g(r)}{4\pi G}\left(y_6^{N-1}(r)+\frac{2}{r}y_5^{N-1}(r)\right)\right]=0. \tag{19}$$

Integrating these equations with respect to the radius r leads to the following:

(1) within the mantle:

$$y_2(r)+2y_4(r)+\frac{g(r)}{4\pi G}\left[y_6(r)+\frac{2}{r}y_5(r)\right]=\frac{A}{r^2};$$

(2) within the fluid core:

$$\frac{g(r)}{4\pi G}\left[y_6^{N-1}(r)+\frac{2}{r}y_5^{N-1}(r)\right]=\frac{B}{r^2};$$

(3) within the inner core:

$$y_2^N(r)+2y_4^N(r)+\frac{g(r)}{4\pi G}\left[y_6^N(r)+\frac{2}{r}y_5^N(r)\right]=\frac{C}{r^2}.$$

Using the boundary conditions (8), (10) and (11), we may write the Consistency Relation at the centre O, the ICB, the CMB and the surface:

$$\begin{cases}\lim\limits_{r\to 0} r^2\left\{y_2^N(r)+2y_4^N(r)+\dfrac{g(r)}{4\pi G}\left[y_6^N(r)+\dfrac{2}{r}y_5^N(r)\right]\right\}=0\\ y_2^N(c)+2y_4^N(c)+\dfrac{g(c)}{4\pi G}\left[y_6^N(c)+\dfrac{2}{c}y_5^N(c)\right]=-P^{ic}+2T^{ic}+\dfrac{g(c)}{4\pi G}\left[y_6^{N-1}(c)+\dfrac{2}{c}y_5^{N-1}(c)\right]\\ y_2(b)+2y_4(b)+\dfrac{g(b)}{4\pi G}\left[y_6(b)+\dfrac{2}{b}y_5(b)\right]=-P^c-2T^c+\dfrac{g(b)}{4\pi G}\left[y_6^{N-1}(b)+\dfrac{2}{b}y_5^{N-1}(b)\right]\\ y_2(a)+2y_4(a)+\dfrac{g(a)}{4\pi G}\left[y_6(a)+\dfrac{2}{a}y_5(a)\right]=-P^e+2T^e\end{cases}. \tag{20}$$

From this system, we may compute the integration constants A, B and C:

$$\begin{cases}C=0\\ B=c^2(P^{ic}-2T^{ic})\\ A=c^2(P^{ic}-2T^{ic})-b^2(P^c+2T^c)\\ A=a^2(-P^e+2T^e)\end{cases}. \tag{21}$$

Note that the surface load S^e and internal load V^{in} disappear in these boundary conditions. The two last conditions involve $a^2(-P^e+2T^e)+b^2(P^c+2T^c)+c^2(-P^{ic}+2T^{ic})=0$, that is the Consistency Relation implies that the total degree-one force acting at the various fluid–solid interfaces and at the surface of the planet has to be equal to zero. Consequently, we have extended the results of Okubo & Endo (1986) to an earth submitted to external and internal pressures and tangential tractions and to internal loading.

In order to do this, we present the analytical solutions for a simple incompressible earth model, first for pressure or tangential traction acting at the surface, the CMB and the ICB, and then for surface and internal loads. The subscript $n=1$ from the previous section will be suppressed for simplicity of notation.

2.2 Particular analytical solutions

2.2.1 External and internal pressure and tangential traction excitation

In this section, the earth model consists of a homogeneous incompressible elastic mantle, an inviscid fluid core and an incompressible elastic inner core. External pressure P^e and tangential traction T^e and internal pressures P^c, P^{ic} and tangential tractions T^c, T^{ic} act at the surface ($r=a$), at the CMB ($r=b$) and at the ICB ($r=c$), respectively. The system of equations is as follows, denoting the solutions within the mantle y_i^1, those within the fluid core y_i^{N-1} and those within the inner core y_i^N:

$$\begin{array}{lll}
y_5^1(a)=0\,, & y_1^1(b)=y_5^{N-1}(b)/g(b)+bK_1\,, & y_1^N(c)=y_5^{N-1}(c)/g(c)-cK_2\,,\\
y_2^1(a)=-P^e\,, & y_2^1(b)-K_1 b\,g(b)\rho^c=-P^c\,, & y_2^N(c)+K_2 c\,g(c)\rho^c=-P^{ic}\,,\\
y_4^1(a)=T^e\,, & y_4^1(b)=-T^c\,, & y_4^N(c)=T^{ic}\,,\\
y_6^1(a)+\dfrac{2}{a}y_5^1(a)=0\,, & y_6^1(b)=y_6^{N-1}(b)-4\pi G\rho^c\,bK_1\,, & y_6^N(c)=y_6^{N-1}(c)+4\pi G\rho^c\,cK_2\,,\\
 & y_5^1(b)=y_5^{N-1}(b)\,, & y_5^N(c)=y_5^{N-1}(c)\,.
\end{array} \tag{22}$$

Solving the 13 first equations leads to solutions in terms of constants. Substituting these solutions into the last equation involves the relation noted in the previous section,

$$a^2(P^e-2T^e)+b^2(-P^c-2T^c)+c^2(P^{ic}-2T^{ic})=0\,.$$

We may compute the deformation as a function of the pressures and tangential traction. Introducing Love numbers, we have the following:

$$\begin{aligned}
y_1(r_o)&=\bar{h}_{r_o}\frac{P^e}{\tilde{\rho}g_o}+\bar{h}^c_{r_o}\frac{P^c}{\tilde{\rho}g_o}+\bar{h}^{ic}_{r_o}\frac{P^{ic}}{\tilde{\rho}g_o}+\tilde{h}_{r_o}\frac{T^e}{\tilde{\rho}g_o}+\tilde{h}^c_{r_o}\frac{T^c}{\tilde{\rho}g_o}+\tilde{h}^{ic}_{r_o}\frac{T^{ic}}{\tilde{\rho}g_o}\,,\\
y_3(r_o)&=\bar{l}_{r_o}\frac{P^e}{\tilde{\rho}g_o}+\bar{l}^c_{r_o}\frac{P^c}{\tilde{\rho}g_o}+\bar{l}^{ic}_{r_o}\frac{P^{ic}}{\tilde{\rho}g_o}+\tilde{l}_{r_o}\frac{T^e}{\tilde{\rho}g_o}+\tilde{l}^c_{r_o}\frac{T^c}{\tilde{\rho}g_o}+\tilde{l}^{ic}_{r_o}\frac{T^{ic}}{\tilde{\rho}g_o}\,,\\
y_5(r_o)&=\bar{k}_{r_o}\frac{P^e}{\tilde{\rho}}+\bar{k}^c_{r_o}\frac{P^c}{\tilde{\rho}}+\bar{k}^{ic}_{r_o}\frac{P^{ic}}{\tilde{\rho}}+\tilde{k}_{r_o}\frac{T^e}{\tilde{\rho}}+\tilde{k}^c_{r_o}\frac{T^c}{\tilde{\rho}}+\tilde{k}^{ic}_{r_o}\frac{T^{ic}}{\tilde{\rho}}\,.
\end{aligned} \tag{23}$$

Because of eq. (13), these Love numbers are not independent and have to be used simultaneously; for example a pressure at the CMB cannot exist alone.

The values of these Love numbers are given in Table 1 for $r_o=a$, $r_o=b$ and $r_o=c$, that is at the surface, the CMB and the ICB, and also for $r=0$. $y_1(0)=y_3(0)$ is the distance between the mass centre of the earth, which is conserved, and the centre of the initial reference sphere, denoted O. Note that, for a homogeneous and incompressible inner core, in the absence of tangential traction acting at the ICB, $y_4^N(c)=0$ and thus $C_3^N=0$; the total displacement within the inner core $y_1^N(r)=C_4^N$ is consequently a rigid translation and thus the distance between the centre O and the mass centre of the earth is equal to the translation at the ICB.

$y_1(a)$ is the translation of the figure centre with respect to the mass centre. If we want to express, for example, the displacement in a reference frame related to the centre of figure, we have to compute $y_1(r)-y_1(a)$ and $y_3(r)-y_1(a)$ using our previous notations.

The pressures at the CMB and ICB have a magnetic origin. From the secular variation of the geomagnetic field, the fluid velocity field at the CMB can be estimated, under the hypothesis of geostrophic motions (Hulot, Le Mouel & Jault 1990) that is assuming a pressure gradient in equilibrium with the Coriolis force. This geostrophic pressure may be easily computed (Gire & Le Mouel 1989; Greff-Lefftz & Legros 1995). Its order of magnitude is around a few hundred pascals and it varies at decade timescales. For example, in 1990 the degree-one magnetic pressure coefficients were (Hulot *et al.* 1990) $p_1^{0c}=-153$ Pa, $p_1^{1c}=246$ Pa and $\tilde{p}_1^{1c}=-31$ Pa. This creates a degree-one displacement with an amplitude on the millimetre scale. It is more difficult to find out the fluid motion and the pressure acting at the ICB (Hulo 1992); the dynamics of the fluid core have to be known (dynamo model).

If the ICB pressure force does not compensate the CMB pressure force, flow within the atmosphere should appear in order to conserve the earth centre of mass. This will create a pressure P^e and a tangential traction T^e cancelling the CMB and ICB pressure force. This flow cannot appear in our equations because we use the static elastogravitational equations; for a more precise investigation, this problem has to be solved using the dynamical equations.

Because of the timescale of the core pressure, decadal pressure and tangential traction should exist within the atmosphere. Note that the most important motions within the atmosphere have a period of less than two years and create a pressure effect and a variation of the thickness of the layer which involves an attraction potential; they consequently act as a surface load and not as a traction in the computations of the deformation of the earth.

Table 1. Degree-one Love numbers (introduced in eq. 23) expressing the radial and tangential displacements and the potential at the surface, the CMB, the ICB and the centre O induced by surface pressure (P^e) and surface tangential traction (T^e) and internal pressure (P^c and P^{ic}) and internal tangential traction (T^c and T^{ic}) acting respectively at the CMB and the ICB.

	$\bar{h}_{r_o}$	$\bar{h}^c_{r_o}$	$\bar{h}^{ic}_{r_o}$	$\tilde{h}_{r_o}$	$\tilde{h}^c_{r_o}$	$\tilde{h}^{ic}_{r_o}$
$r_o=a$	−0.5629	0.1392	0.0	1.2418	0.3417	0.0
$r_o=b$	−0.2661	0.2002	0.0	0.0447	0.1342	0.0
$r_o=c$	30.310	−8.983	−6.172	−60.86	−18.099	12.345
$r_o=0$	30.310	−8.983	−6.172	−60.86	−18.099	12.211

	$\bar{l}_{r_o}$	$\bar{l}^c_{r_o}$	$\bar{l}^{ic}_{r_o}$	$\tilde{l}_{r_o}$	$\tilde{l}^c_{r_o}$	$\tilde{l}^{ic}_{r_o}$
$r_o=a$	−0.7415	0.1024	0.0	2.3064	0.4046	0.0
$r_o=b$	−0.5931	0.1330	0.0	1.1557	0.5509	0.0
$r_o=c$	30.310	−8.983	−6.172	−60.86	−18.099	12.479
$r_o=0$	30.310	−8.983	−6.172	−60.86	−18.099	12.211

	$\bar{k}_{r_o}$	$\bar{k}^c_{r_o}$	$\bar{k}^{ic}_{r_o}$	$\tilde{k}_{r_o}$	$\tilde{k}^c_{r_o}$	$\tilde{k}^{ic}_{r_o}$
$r_o=a$	0.	0.	0.	0.	0.	0.
$r_o=b$	1.2740	−0.3150	0.	−2.8106	−0.7735	0.
$r_o=c$	13.588	−4.027	0.	−27.284	−8.1136	0.
$r_o=0$	0	0	0	0	0	0.

The atmospheric pressure has been well known for 10 years, so it could be interesting to try to find a decadal degree-one term in these data in order to show correlation with internal pressure. Nevertheless, it seems more physically likely that there is an equilibrium among the tractions within the core (that is among P^c, T^c, P^{ic} and T^{ic}) and that the atmosphere tractions are disconnected from the fluid-core motion.

2.2.2 *Internal and surface load excitation*

A superficial mass distribution located at the radius r_o produces a pressure P^{in} effect and a potential V^{in} effect (see section 2.1.2). The total resulting force is equal to zero and after having solved the first $6N-3$ equations, the last equation will become $0=0$. We first investigate the deformation induced by these excitation sources for a homogeneous earth model.

Homogeneous elastic sphere. For this simplest case, noting S^e the surface-loading potential, we have to solve the equations

$$\begin{aligned}
&y_5^1(a)=0, && y_1^1(r_o)=y_1^2(r_o),\\
&y_2^1(a)=-\rho S^e, && y_2^1(r_o)=y_2^2(r_o)+\frac{g(r_o)}{g_o}\frac{a}{r_o}\rho V^{in},\\
&y_4^1(a)=0, && y_4^1(r_o)=y_4^2(r_o),\\
&y_6^1(a)+\frac{2}{a}y_5^1(a)=\frac{3}{a}S^e, && y_6^1(r_o)=y_6^2(r_o)-3\frac{V^{in}}{r_o},\\
& && y_5^1(r_o)=y_5^2(r_o),\\
& && y_3^1(r_o)=y_3^2(r_o).
\end{aligned} \tag{24}$$

The solutions may be written as follows for an incompressible homogeneous sphere:

$$y_1^1(a)=-\frac{S^e}{g_o}-\left(\frac{r_o}{a}\right)^2\frac{V^{in}}{g_o}, \qquad y_3^1(a)=-\frac{S^e}{g_o}-\left(\frac{r_o}{a}\right)^2\left[1-\frac{\rho g_o a}{6\mu}\left(1-\left(\frac{r_o}{a}\right)^2\right)\right]\frac{V^{in}}{g_o}. \tag{25}$$

Note that the elastic parameter (rigidity μ) does not appear in the solutions for a surface load: an incompressible homogeneous body submitted to a degree-one surface load has the same behaviour as a non-deformable body. This remark would not be true for a compressible homogeneous body: taking the fundamental solutions of the y_i system for a compressible homogeneous body (Love 1911), and solving the boundary conditions, the y_i solutions are dependent on the elastic parameters. There is a

non-negligible difference between compressible and incompressible loading Love numbers for a homogeneous sphere; taking $\mu=1.45\times10^{11}$ Pa, $\lambda=3\times10^{11}$ Pa and $\rho=5520$ kg m^{-3} as mean values for the Earth, we obtain, for a surface load in a homogeneous earth,

$$y_1^1(a)=-1.212\frac{S^e}{g_o} \qquad \text{and} \qquad y_3^1(a)=-0.833\frac{S^e}{g_o}. \tag{26}$$

These values express the displacement in a frame related to the mass centre.

Comparison with Farrell's Love numbers. In this paper, the displacement is expressed in a frame related to the mass centre and consequently the associated Love numbers appear to be in disagreement with those of Farrell (1972) and Merriam (1985). This is because Farrell (1972) chose the centre of mass of the undeformed earth for the origin of his reference frame. If the earth is rigid, a surface load S^e will involve a shift of the centre of mass (with respect to the centre of mass of the initial sphere) which may be computed from the MacCullagh theorem (see also Mitrovica, Davis & Shapiro 1994a):

$$u_o=\frac{S^e}{g_o}. \tag{27}$$

Consequently, there is only a translation u_o between the reference frame used by Farrell and the reference frame related to the centre of mass of the deformed earth (this paper), which is conserved and remains coincident with the initial reference sphere centre of mass. Farrell's Love numbers (denoted superscript F) are thus defined, using our notation, as

$$\begin{cases} y_1(a)+\dfrac{S^e}{g_o}=h_a'^F\dfrac{S^e}{g_o}, & \text{with} \quad h_a'^F=-0.290, \\ y_3(a)+\dfrac{S^e}{g_o}=l_a'^F\dfrac{S^e}{g_o}, & \text{with} \quad l_a'^F=0.113, \\ y_5(a)+S^e=k_a'^F S^e, & \text{with} \quad k_a'^F=0; \end{cases} \tag{28}$$

we thus have simple relations between our Love numbers and those of Farrell:

$$h_a'^F=1+h_a', \qquad l_a'^F=1+l_a' \qquad \text{and} \qquad k_a'^F=1+k_a'. \tag{29}$$

Realistic compressible earth model. For the PREM compressible earth model, using a Runge–Kutta numerical integration, our approach, where the origin of the reference frame is the centre of mass of the deformed earth itself, gives a displacement at the earth's surface

$$y_1^1(a)=-1.2858\frac{S^e}{g_o}$$

and

$$y_3^1(a)=-0.8958\frac{S^e}{g_o}.$$

Adding $+1$ to these values allows us to obtain the Love numbers computed by Farrell (1972). We may also compute the shift of the centre of the initial reference sphere O with respect to the centre of mass for the PREM compressible earth model:

$$y_1^N(0)=y_3^N(0)=-0.39576\frac{S^e}{g_o}.$$

To conclude, in using the degree-one Love numbers it is necessary to be careful about the definition of the Love numbers and the chosen reference frame, especially its origin, that is whether it is related to the mass centre of the deformed Earth (this paper) or the undeformed Earth (Farrell 1972; Merriam 1985; Wu 1990) and whether it is related to the centre of figure or the surface of the planet (for geodetic measurements, the stations are located at the earth's surface).

Degree-one deformation induced by atmospheric loading. We investigate the elastic deformation induced by a surface-loading potential S^e using the PREM compressible earth model. Solving the boundary conditions numerically, the solutions may be written

$$y_1(r_o)=h'_{r_o}\frac{S^e}{g_o} \qquad \text{and} \qquad y_3(r_o)=l'_{r_o}\frac{S^e}{g_o}. \tag{30}$$

The values of these Love numbers are given in Table 2 for $r_o=a$, $r_o=b$ and $r_o=c$, that is at the surface, the CMB and the ICB, and also for $r=0$, the centre of the initial reference sphere.

Taking the time-dependent zonal and sectorial degree-one continental-loading potential within the atmosphere [computed by Gegout (1995) from an 8 yr pressure-field record provided by ECMWF in Reading (UK)] shown in Fig. 2(a), we can compute, for

Table 2. Degree-one loading Love numbers (introduced in eq. 30) induced by a surface load, expressing the radial and tangential displacements at the surface, the CMB, the ICB and the centre *O*.

	h'_{r_o}	$l'^{c}_{r_o}$
$r_o = a$	−1.28585	−0.89590
$r_o = b$	−1.03481	−0.99641
$r_o = c$	−0.39583	−0.39583
$r_o = 0$	−0.39583	−0.39583

this three-layered model, the radial displacement at the surface (Fig. 2b), at the CMB (Fig. 2c) and at the ICB (Fig. 2d) as a function of time. For this computation, we use the Love numbers computed above. This result is not perfect because we do not take into account the effect of variations of the water thickness induced by the deformation of the bottom of the oceans [coefficient $1/\beta_1$, with $\beta_1 = 1-(\rho^w/\bar{\rho})(1+k'_a-h'_a)$, where ρ^w is the water density, introduced by Gegout (1995) and Gegout & Legros (1997)]. The amplitude of the deformations will be amplified by a factor $1/\beta_1$, that is by about 30 per cent. These displacements vary of course, with periods of less than two years and orders of magnitude of a few millimetres.

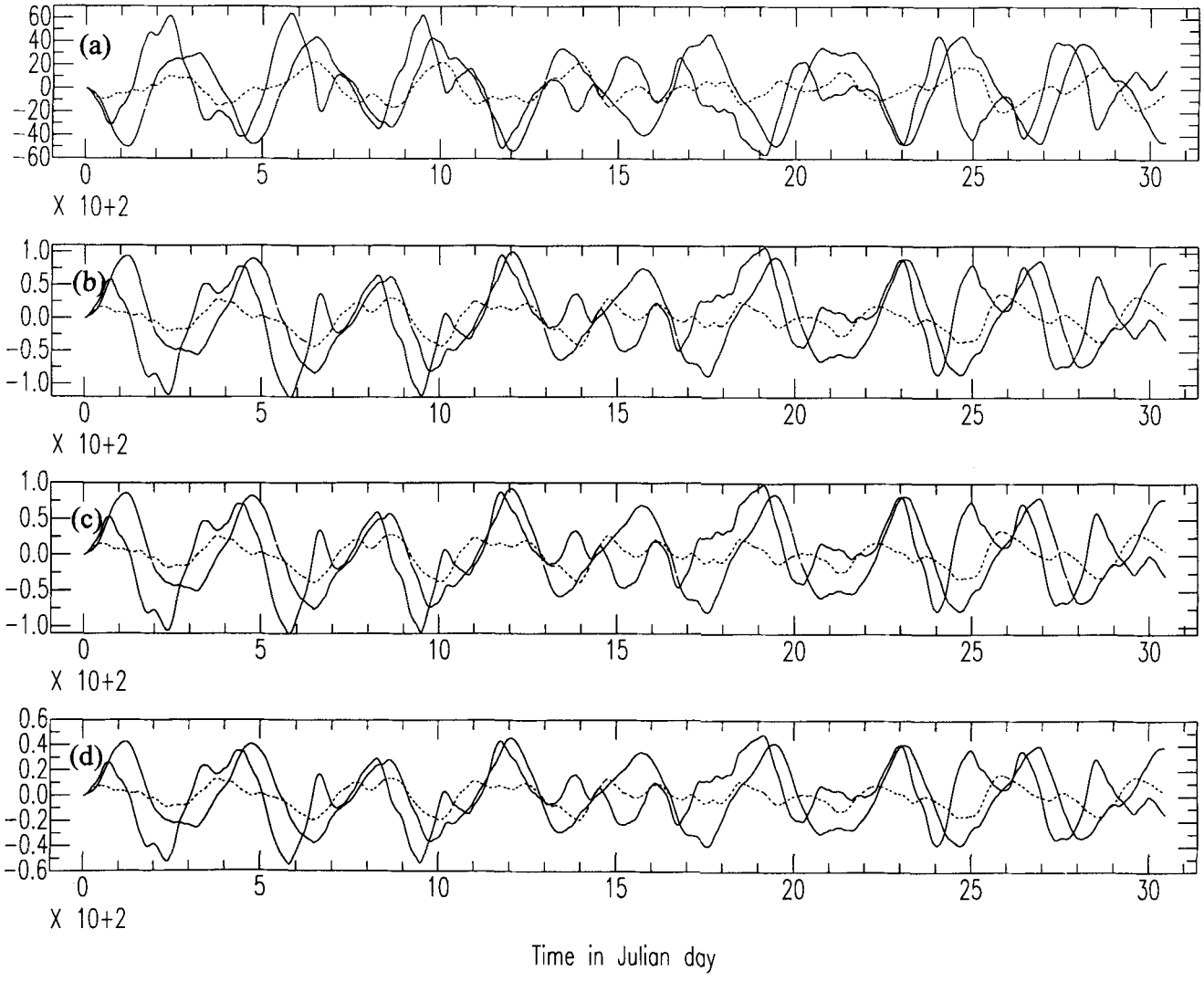

Figure 2. (a) Time-dependent zonal (solid line) and sectorial (cosine term shown by dashed line and sine term by dotted line) degree-one continental loading originating from an eight-year pressure-field record provided by the European Centre for Medium Range Weather Forecasts (ECMWF) in Reading (UK). (b) Radial displacement at the earth's surface induced by the continental loading described in (a). (c) Radial displacement at the CMB induced by the continental loading described in (a). (d) Radial displacement at the ICB induced by the continental loading described in (a).

3 VISCOELASTIC THEORY

In the previous section we computed the elastic deformation of the Earth induced by degree-one excitation sources varying in timescale from a year to several decades. At larger timescales, we have to take into account the viscous response of the Earth. To do that we have chosen as the rheological law a linear viscoelastic Maxwell model of rheology. This is because at short timescales the Earth has an elastic behaviour, and at intermediate timescales (10^3–10^6 years) it shows viscous relaxation (for example the Pleistocene deglaciation), whereas at long (geological) timescales its behaviour is characterized by that of a fluid (the flattening of the Earth is quasi-hydrostatic and is explained by fluid rotation). In the frequency domain, the stress–strain relation for an incompressible Maxwell body is the Hookean law, but the rigidity μ^i is a function of the frequency λ:

$$\mu^i(\lambda)=\mu^{ie}\frac{i\lambda}{i\lambda+\mu^{ie}/\nu^i},$$

where μ^{ie} is the elastic rigidity and ν^i the Newtonian viscosity of layer i. In the Fourier domain, the viscoelastic equations and the boundary conditions are the same as those for an elastic body with the same geometry. Consequently, we may use the correspondence principle: we solve the elastic problem for different frequencies in order to build the viscoelastic solutions (Peltier 1974; Wu & Peltier 1982).

The viscoelastogravitational equations are the $6N-3$ equations described in Section 2, taking into account the conservation of the centre of mass; the frequency dependence comes from the viscoelastic stress $y_2^i(r)$ and $y_4^i(r)$. Before solving this set of $6N-3$ equations, we compute the determinant of the system, and we find a frequency-dependent polynomial whose zeros are called relaxation modes (e.g. Peltier 1974; Wu & Peltier 1982; Yuen & Peltier 1983; Han & Wahr 1995; Vermeesen, Sabadini & Spada 1996).

3.1 Relaxation modes

For deformation of degree $n > 1$, it is well known that these relaxation modes are generated at each interface by the discontinuity of physical parameters. For example, for a five-layered model consisting of an elastic lithosphere, a viscoelastic upper and lower mantle, an inviscid fluid core and a viscoelastic inner core, we have seven relaxation modes (Peltier 1974; Spada *et al.* 1992; Lefftz & Legros 1993):

M_o due to the surface discontinuity at $r=a$; M_1 due to the density jump between the upper and the lower mantle;

C and G because of the density discontinuity between the fluid core and the lower mantle and between the fluid core and the inner core;

L due to the viscosity contrast between the elastic lithosphere and the upper mantle; T_1 and T_2 due to a jump in rigidity or viscosity distribution between the upper and the lower mantle, called transition modes because they relax rapidly and are weakly excited.

In this section we wish to investigate the degree-one relaxation modes. Because the initial system of boundary conditions degenerates, the number of modes should be different. To understand their origin, we start with simple models (homogeneous sphere, two layers, etc.).

3.1.1 Homogeneous incompressible sphere

For an incompressible homogeneous earth, the equations are (*cf.* eq. 24):

$$\begin{aligned} &y_5^1(a)=0,\\ &y_2^1(a)=-\tilde{\rho}S^e,\\ &y_4^1(a)=0. \end{aligned} \tag{31}$$

The discontinuity of the gravity field $y_6^1(a)+(2/a)y_5^1(a)=(3/a)S^e$ will be verified after resolving this system.

Taking

$$\mu(\lambda)=\mu^e\frac{i\lambda}{i\lambda+\mu^e/\nu},$$

where μ^e is the elastic rigidity, ν is the Newtonian viscosity of the sphere and $\tau=\nu/\mu^e$ is the Maxwell relaxation time of the mantle, the determinant of the system of the three independent equations may be written as follows:

$$\det=3\mu^e a^2\rho g_o\frac{i\lambda\tau}{1+i\lambda\tau}. \tag{32}$$

This determinant is equal to zero for $i\lambda=0$ (that is the fluid limit): there is no relaxation mode for a homogeneous incompressible sphere. This is because the solution of the system is the rigid translation (only $C_4^1\neq 0$, and thus the strains vanish): a homogeneous incompressible planet has the same behaviour as a non-deformable body.

Note that for degree $n > 1$, the determinant cancels for

$$i\lambda = -\frac{1}{\left[1+\dfrac{2n^2+4n+3}{n}\dfrac{\mu^e}{\rho g_o a}\right]\tau},$$

the M_o mode (e.g. Wu & Peltier 1982). Substituting n by 1 in the last equation has no meaning, because the system of boundary conditions is different. We may conclude that for degree one the M_o mode does not exist.

3.1.2 Two-layered earth model

In this part we introduce an inviscid fluid core within the viscoelastic mantle. For this model, where $s=b/a$, the determinant cancels for

$$i\lambda = 0 \quad \text{and} \quad i\lambda = -\frac{\beta s^2(1-s)}{\left[3(1+\beta s^3)\dfrac{\mu^e}{\rho g_o a}+\beta s^2(1-s)\right]\tau}. \tag{33}$$

This mode is proportional to β, the density contrast between the fluid core and the mantle, and will disappear if β tends to zero: this is the C mode. Taking the mean averaged values for the density of the mantle (4414 kg m^{-3}) and of the core (12400 kg m^{-3}), a mantle rigidity $\mu^e = 0.166\times10^{12}$ Pa and viscosity $\nu = 10^{21}$ Pa s leads to a relaxation time τ_c associated with C of about 2300 yr.

3.1.3 Three-layered earth model

The earth consists of a viscoelastic homogeneous inner core, an inviscid fluid core and a viscoelastic mantle. Where the density contrast between the inner core and the fluid core is β_g, and $s_g = c/a$, we show that the determinant cancels for

$$i\lambda = 0 \quad \text{and} \quad i\lambda = -\frac{\beta(s^3+\beta s^3+\beta_g s_g^3)(1-s)}{\left[3(1+\beta)s(1+\beta s^3+\beta_g s_g^3)^2\dfrac{\mu^e}{\rho g_o a}+\beta(s^3+\beta s^3+\beta_g s_g^3)(1-s)\right]\tau}. \tag{34}$$

This is the C mode because it is proportional to β. There is no relaxation mode related to the density contrast between the inner core and the fluid core (because the inner core is homogeneous and a homogeneous incompressible sphere does not create a relaxation mode). Consequently, for degree one, the G mode does not exist.

3.1.4 Four-layered earth model

We want to investigate the mode created by an elastic–viscoelastic interface. To do that we introduce a homogeneous elastic lithosphere in the previous model. The determinant will cancel for zero, for the C mode, and also for another mode, which depends on the viscosity of the mantle and does not disappear if the density contrast between the lithosphere and the mantle tends to zero: this is the L mode.

3.1.5 Five-layered earth model

If we introduce a viscoelastic–viscoelastic interface (to describe the upper-mantle–lower-mantle boundary), we can show that it creates two other modes. The largest one depends on the viscosity of the mantle and exists even if the density contrast between the two layers is zero; it is similar to the transition modes T_1 and T_2. The second one is proportional to the density contrast between the upper and lower mantle and its value depends on the viscosities of these layers; this is the M_1 mode. The difference between degree one and degree $n > 1$ is the transition mode: for degree one there is only one transition mode instead of two.

In conclusion, for the five-layered earth model described in Table 3(a), there are only four degree-one relaxation modes (T, C, L, M_1) instead of seven (T_1, T_2, M_o, C, L, M_1, G) for the other degrees. Their values are given in Table 3(b), and we show the relaxation modes of this earth model in Fig. 3 as a function of the degree n (Greff-Lefftz & Legros 1996).

3.2 Viscoelastic Love numbers

For a Maxwell model of rheology, Peltier (1974) and, more recently, Spada *et al.* (1990) have shown that the viscoelastic Love numbers have the following frequency form [for example $h(\lambda)$]:

$$h(\lambda) = h^e + \sum_{i=1}^{M}\frac{h^i}{i\lambda+1/\tau_i}. \tag{35}$$

Table 3. (a) Geometrical and physical parameters for a five-layered model consisting of an elastic lithosphere, a viscoelastic upper mantle, a viscoelastic lower mantle, an inviscid fluid core and a viscoelastic inner core. Both rigidity and density are obtained from PREM (Dziewonski & Anderson 1981). (b) Four degree-one relaxation modes associated with the viscoelastic Love numbers for the five-layered model described in (a).

(a)	Radius (km)	Density (kg m^{-3})	Rigidity (Pa)	Viscosity (Pa s)
	$a_1=6221<r<a$	$\rho_1=3232$	$\mu_1=6.114\times10^{10}$	$\nu_1=\infty$
	$a_2=5701<r<a_1$	$\rho_2=3666$	$\mu_2=9.169\times10^{10}$	$\nu_2=2\times10^{21}$
	$a_3=3480<r<a_2$	$\rho_3=4904$	$\mu_3=2.225\times10^{11}$	$\nu_3=8\times10^{22}$
	$a_4=1225.5<r<a_3$	$\rho_4=10901$	$\mu_4=0$	$\nu_4=0$
	$0<r<a_4$	$\rho_5=12894$	$\mu_5=1.644\times10^{11}$	$\nu_5=10^{13}$

(b)	Relaxation modes (s^{-1})	Relaxation times (kyr)
T	-0.427×10^{-10}	0.742
C	-0.465×10^{-12}	68.107
L	-0.137×10^{-12}	230.885
M_1	-0.267×10^{-14}	11781.87

The first term on the right, h^e, is the instantaneous elastic Love number and τ_i and h^i are the relaxation times and residues of the M modes of the earth model. h^i depends on the excitation sources.

For degree one, the form is conserved and only the number of relaxation modes changes. In the temporal domain, these Love numbers will be written

$$h(t)=h^e\delta(t)+\sum_{i=1}^{M}h^i e^{-t/\tau_i}H(t)\,. \tag{36}$$

For surface and internal loads we have computed the degree-one deformation in radial displacement and in equipotential (at each interface a_i of the earth model) induced by unit constant internal-mass distribution [$\sigma=H(t)$ kg m^{-2}], located at radius r_o, that is for a loading potential

$$V^{in}=g_o r_o\frac{H(t)}{\tilde{\rho}a}:$$

$$y_1(a_i)=h'_{a_i}(t)*\frac{r_o}{\tilde{\rho}a}H(t)\qquad\text{and}\qquad \frac{y_5(a_i)}{g_o}=\begin{cases}\left[\dfrac{a_i}{r_o}\delta(t)+k'_{a_i}(t)\right]*\dfrac{r_o}{\tilde{\rho}a}H(t) & \text{if } a_i\le r_o\,,\\[2ex] \left[\left(\dfrac{r_o}{a_i}\right)^2\delta(t)+k'_{a_i}(t)\right]*\dfrac{r_o}{\tilde{\rho}a}H(t) & \text{if } a_i\ge r_o\,.\end{cases} \tag{37}$$

These deformations are shown in Fig. 4 for the topography and Fig. 5 for the equipotential at the surface, at the 670 km depth discontinuity, at the CMB and at the ICB (a, b, c and d, respectively), as a function of r_o and of time.

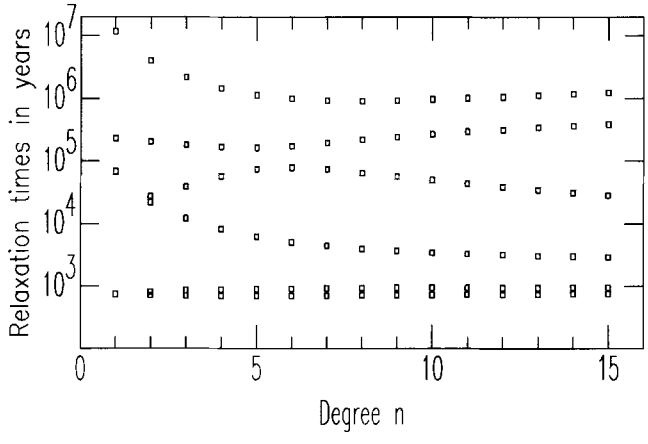

Figure 3. Relaxation times of the earth model described in Table 3(a) in years, as a function of the degree n.

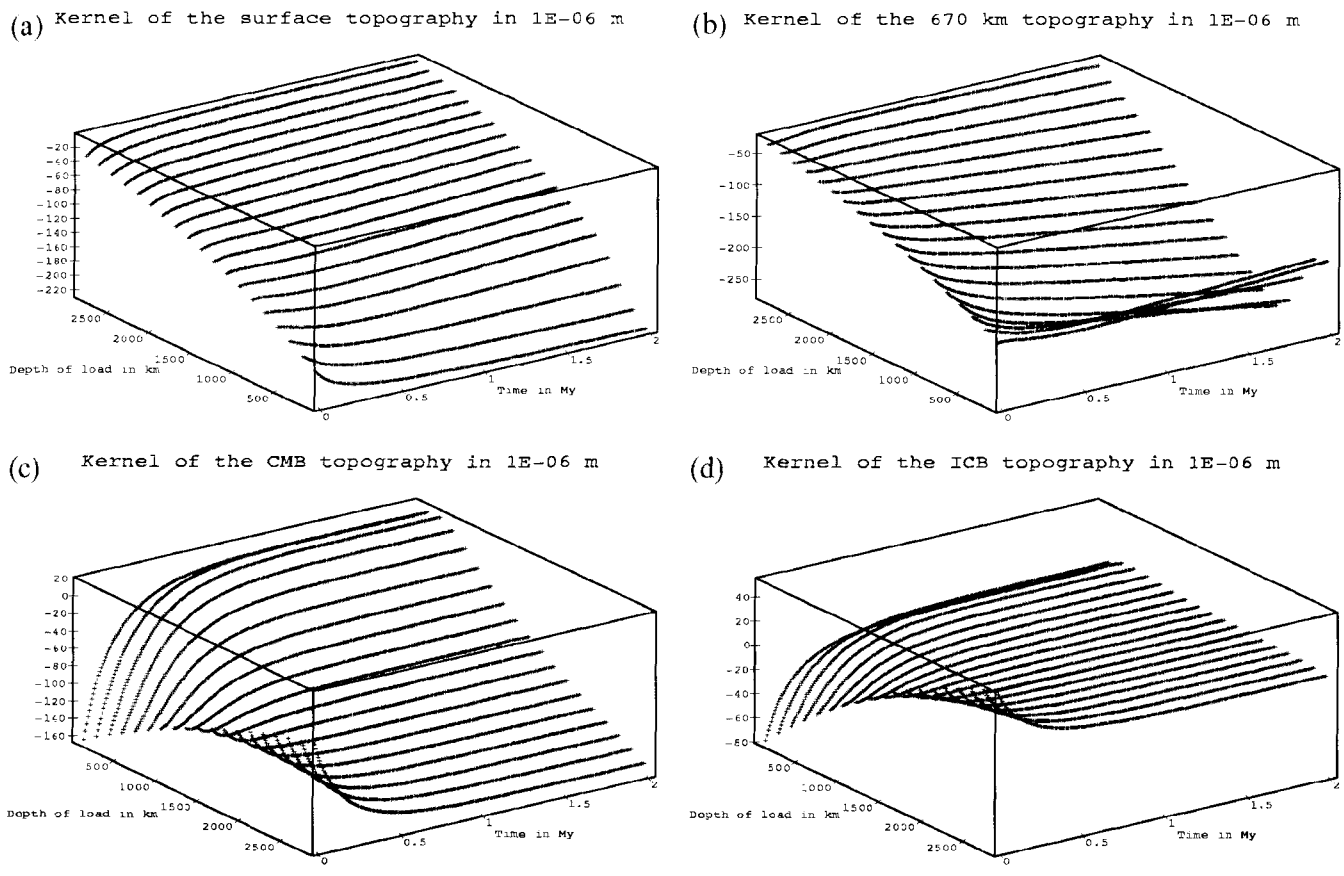

Figure 4. Topography in 10^{-6} m at the surface (a), at the 670 km depth discontinuity (b), at the CMB (c) and at the ICB (d) induced by a unit internal load as a function of time and of the depth of the load.

For a geophysical application, we present the degree-one topography induced by the Pleistocene deglaciation. This glaciation–deglaciation is modelled simply by three spherical ice sheets (e.g. Peltier & Wu 1983; Wu & Peltier 1984) analytically expanded in spherical harmonics (e.g. Farrell 1972) and with a time dependence (shown in Fig. 6a) such that the surface mass distribution $\sigma_1(t)$ can be written (Peltier, Drummond & Tushingham 1986)

$$\sigma_1(t)=\frac{\sigma_1^o}{T}\left[R(t)-\frac{T_1}{T_1-T_o}R(t-T_o)+\frac{T_o}{T_1-T_o}R(t-T_1)\right], \tag{38}$$

where $R(t)$ is the ramp function, the glaciation is characterized by a slow build-up over a period $T_o=90\,000$ years and the deglaciation by a fast collapse lasting $T_1-T_o=10\,000$ years (see Fig. 6a). The parameters (that is the radius, the latitude and the longitude of the centre of the spherical cap) for the Fennoscandian, Canadian and Antartic ice sheets are taken from Table 3 of Spada *et al.* (1992); from the ice-height and sea-level change we compute the degree-one term of such a density anomaly:

$$\sigma_{10}^o=0.112\times10^6\ \mathrm{kg\ m^{-2}},\qquad \sigma_{11}^o=0.291\times10^5\ \mathrm{kg\ m^{-2}},\qquad \text{and}\qquad \tilde{\sigma}_{11}^o=-0.308\times10^5\ \mathrm{kg\ m^{-2}}. \tag{39}$$

In Fig. 6(b) we present the temporal evolution of the surface, the 670 km depth discontinuity, the CMB and the ICB degree-one topographies induced by the degree-one term of the glaciation–deglaciation: these topographies are translation maximal in the directions

$$\cos\theta_o=\frac{\sigma_{10}^o}{[\sigma_{10}^{o2}+\sigma_{11}^{o2}+\tilde{\sigma}_{11}^{o2}]^{1/2}}$$

and

$$\tan\varphi_o=\frac{\tilde{\sigma}_{11}^o}{\sigma_{11}^o},$$

that is $\theta_o=20.7°$ and $\varphi_o=-46.6°$, θ_o being the colatitude and φ_o the longitude. Note that the amplitudes of these deformations are

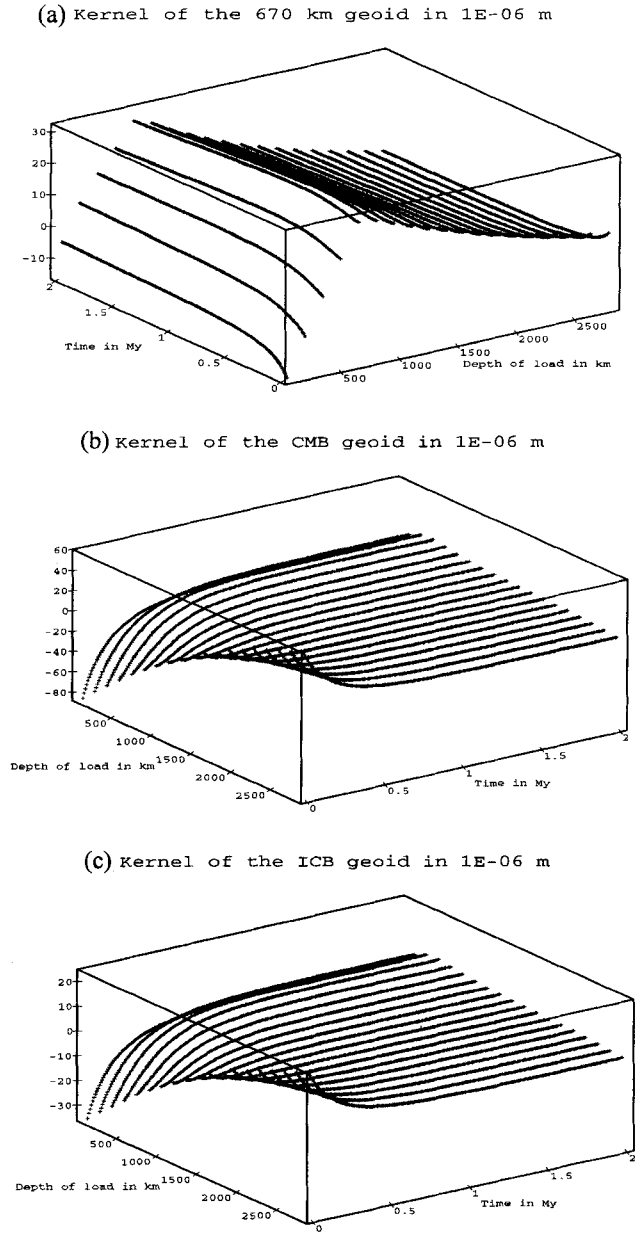

Figure 5. Equipotential in 10^{-6} m at the surface (a), at the 670 km depth discontinuity (b), at the CMB (c) and at the ICB (d) induced by a unit internal load as a function of time and of the depth of the load.

about 10 m (Wu 1990). At present, that is almost 7000 yr after the end of the deglaciation, the displacements are

$y_1(a) = -1.36$ m, $y_1(5701\text{ km}) = -0.38$ m, $y_1(b) = 5.35$ m and $y_1(c) = 2.44$ m;

$y_3(a) = -2.83$ m, $y_3(5701\text{ km}) = -6.48$ m, $y_3(b) = -1.06$ m and $y_3(c) = 2.44$ m.

The present-day distance between the geometric centre of the inner core and the mass centre is consequently about 2.44 m.

In Figs 6(c) and (d) we have calculated the present rate of the radial and tangential surface displacements, that is $\dot{y}_1(a)\,Y_1(\theta, \varphi)$ and $\dot{y}_3(a)\nabla_H Y_1(\theta, \varphi)$, where $\dot{}$ denotes the time derivative. In the direction of the maximal translation (θ_o, φ_o), we obtain the maximum deformation rate of the radial displacement $\dot{y}_1(a) = 0.14$ mm yr^{-1}, and in the direction $(\theta_o + \Pi/2, \varphi_o)$ the maximum amplitude of the tangential displacement vector is $\dot{y}_3(a) = 0.64$ mm yr^{-1}. Notice that in the direction (θ_o, φ_o) and at the antipode, the tangential displacement vector is equal to zero; this is a consequence of the degree-one symmetry (Mitrovica *et al.* 1994a,b; Mitrovica & Davis 1995).

For these computations, we have taken the five-layered earth model described in Table 3(a), but with an upper-mantle viscosity of about 10^{21} Pa s and a lower-mantle viscosity of about 5×10^{21} Pa s, because this viscosity profile agrees with various glaciation data (e.g. Mitrovica & Peltier 1993). As shown in Fig. 12(c) of Wu (1990), the amplitude of the CMB topography induced by a surface load is very sensitive to the viscosity profile within the mantle, because of the combination of the relaxations of the different interfaces of the earth model.

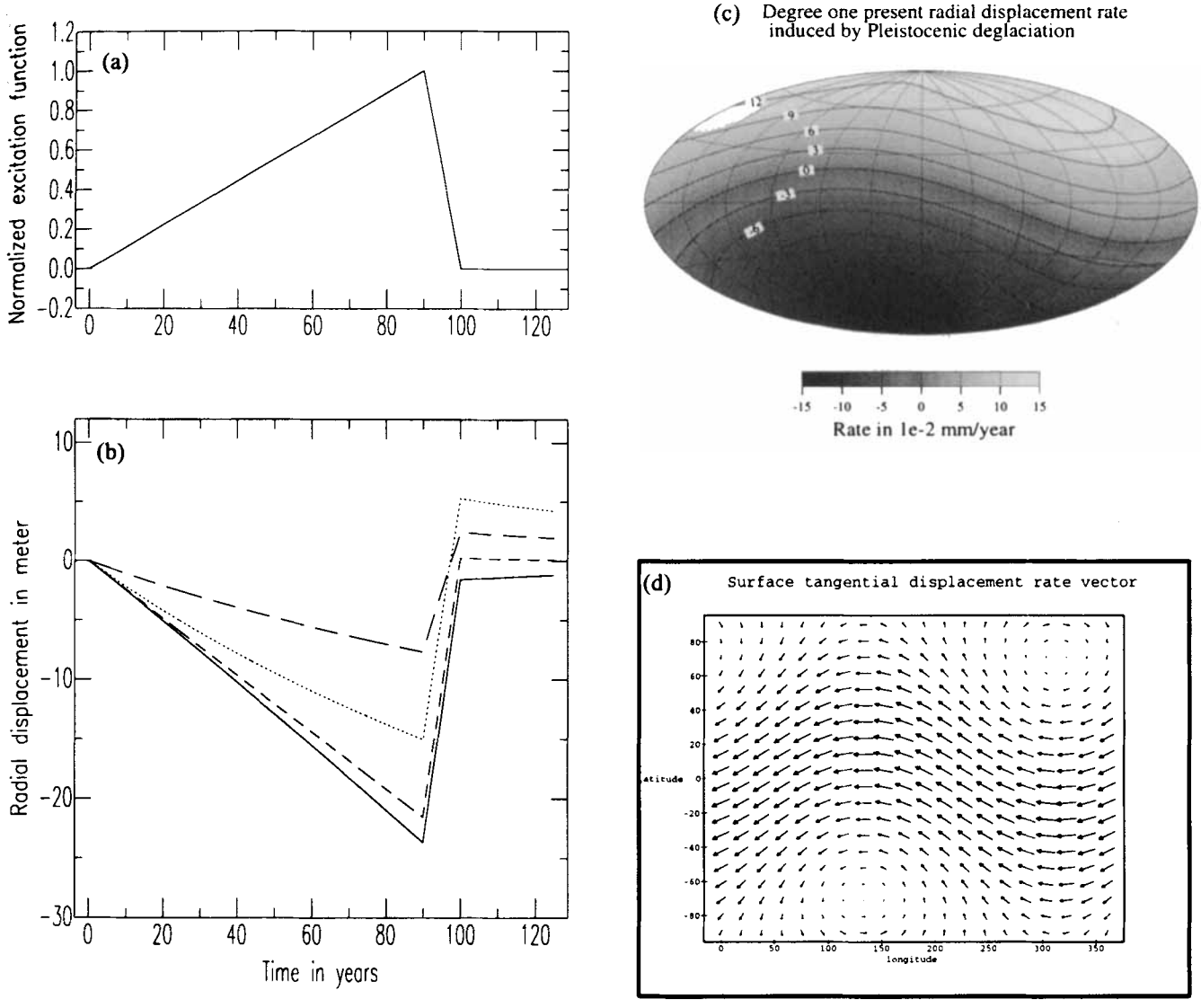

Figure 6. (a) Time dependence of the glaciation model described in eq. (38). The glaciation is characterized by a slow build-up for 90 000 yr and the deglaciation by a fast collapse lasting 10 000 years. The present day is almost 7000 yr after the end of the deglaciation. (b) Surface topography (solid line), 670 km interface (short-dashed line), CMB (dotted line) and ICB (dashed line) induced by the glaciation–deglaciation model described in (a) as a function of time. (c) Present-day surface radial displacement rate. The contour interval is 2×10^{-2} mm yr^{-1}. The maximum amplitude is in the direction $\theta_o = 20.7°, \varphi_o = 313.4°$. (d) Present-day surface tangential displacement vector rate. The maximum amplitude is about 0.64 mm yr^{-1} and is at $\theta_o + \Pi/2, \varphi_o$.

3.3 Quasi-fluid approximation

The timescale of the temporal evolution of the internal load is that of the convection. Consequently, the time t is larger than the relaxation times τ_i of the viscoelastic deformation and we may carry out some limited expansion in the Love numbers in the frequency domain for $i\lambda\tau_i \ll 1$:

$$h'(\lambda) = \left[h'^{e} + \sum_{i=1}^{M} h^i \tau_i\right] - i\lambda \sum_{i=1}^{M} h^i \tau_i^2, \tag{40}$$

or in the temporal domain:

$$h'(t) = \left[h'^{e} + \sum_{i=1}^{M} h^i \tau_i\right] \delta(t) - \sum_{i=1}^{M} h^i \tau_i^2 \, \delta'(t). \tag{41}$$

The first term in the square bracket is the fluid limit of the loading Love number h'^{f}, whereas the second term takes into account the

past, that is the viscous response of the earth. In this quasi-fluid approximation, the Maxwell body is equivalent to a Newtonian body [taking $\mu(\lambda) \simeq i\lambda\nu$].

We compute for this quasi-fluid approximation the degree-one deformation in topography and equipotential induced by a constant internal mass distribution [$\sigma = H(t)$ kg m^{-2}], located at a radius r_o, that is for a loading potential $V^{in} = g_o(r_o/a)(H(t)/\tilde{\rho})$, for $t > 0$,

$$y_1^f(a_i) = \left(h'^e_{a_i} + \sum_{k=1}^{M} h^k_{a_i} \tau_k \right) \frac{r_o}{\tilde{\rho} a} H(t), \tag{42}$$

$$\frac{y_5^f(a_i)}{g_o} = \begin{cases} \left[\dfrac{a_i}{r_o} + k'^e_{a_i} + \displaystyle\sum_{k=1}^{M} k^k_{a_i} \tau_k \right] \dfrac{r_o}{\tilde{\rho} a} H(t) & \text{if } a_i \le r_o, \\ \left[\left(\dfrac{r_o}{a_i} \right)^2 + k'^e_{a_i} + \displaystyle\sum_{k=1}^{M} k^k_{a_i} \tau_k \right] \dfrac{r_o}{\tilde{\rho} a} H(t) & \text{if } a_i \ge r_o . \end{cases} \tag{43}$$

These are the deformations remaining just after the viscoelastic relaxation (i.e. $t > \tau_i$) and they are equivalent to Newtonian deformations (e.g. see Forte *et al.* 1993).

The topographies and the equipotentials are represented in Figs 7 and 8, respectively. Two cases have been investigated: in Figs 7(a) and 8(a) the five-layered model has a density contrast between the upper and lower mantle (denoted β_m), that is there is an M_1 relaxation mode, whereas in Figs 7(b) and 8(b) the mantle is assumed homogeneous (there is no M_1 mode). The problem of the existence of such a density contrast at 670 km depth is important for the surface topography because an internal load located within the lower mantle induces positive topography at the earth's surface if $\beta_m \neq 0$ and negative topography if $\beta_m = 0$.

For a viscosity contrast of about 40 between the upper and lower mantle, a positive mass anomaly within the upper mantle creates a weak negative topography at the CMB, whereas mass anomaly within the lower mantle involves a larger positive CMB topography. The sign of the deformation (positive or negative) for a mass anomaly located in the upper mantle is strongly dependent on the viscosity profile within the mantle and on the existence of a density jump at 670 km depth. In any case, the amplitude of the CMB topography is larger for mass anomalies located in the lower mantle than in the upper mantle.

Note that the ICB is in a quasi-hydrostatic equilibrium, that is $g(c)\, y_1^N(c) = y_5^N(c)$, whatever the value of r_o. This is a consequence of the low viscosity of the inner core (about 10^{13} Pa s.), which means that the inner-core behaviour is closed to that of a hydrostatic

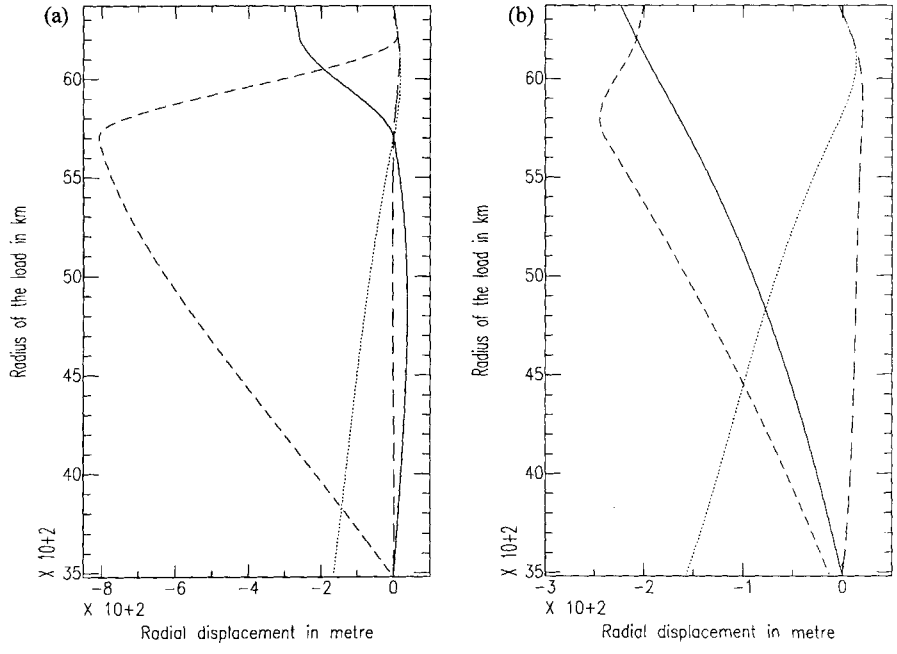

Figure 7. Radial displacement at the surface (solid line), at the 670 km depth discontinuity (short-dashed line), at the CMB (dotted line) and at the ICB (dashed line) induced by a unit internal load as a function of the radius of the load, that is its location within the mantle, in the quasi-fluid approximation. The five-layered earth model used has a density contrast $\beta_m \neq 0$ at 670 km depth (b) and $\beta_m = 0$ (a).

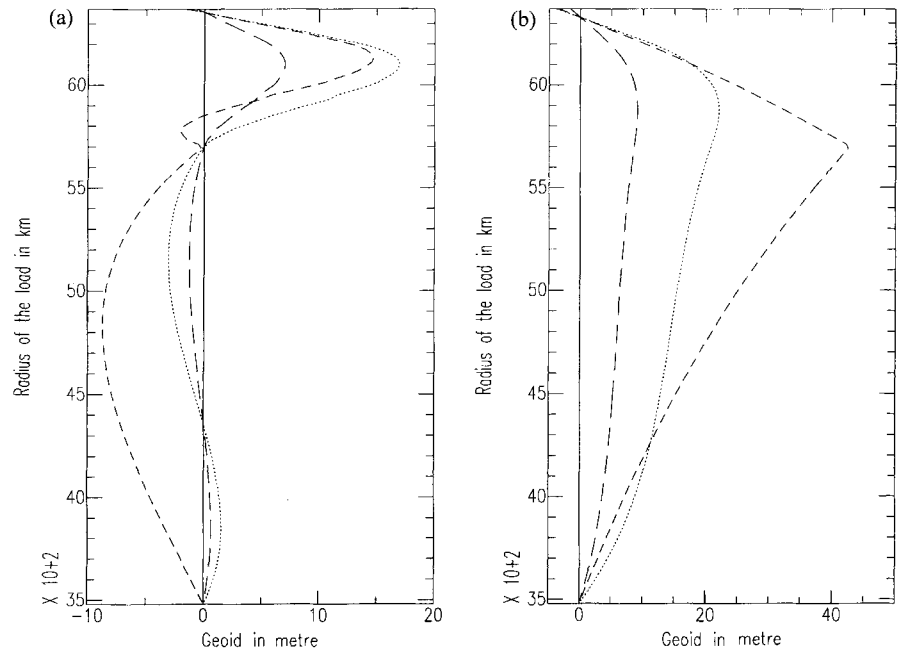

Figure 8. The same as Fig. 7 for the equipotential.

fluid. On the another hand, the internal loads within the mantle are partly isostatically compensated at the CMB, which explains the low amplitude of the ICB deformation.

In the absence of tangential traction acting at the ICB and for a homogeneous and incompressible inner core, $y_1^N(c)$ is equal to $y_1^N(0)$ and thus represents the distance between the geometric centre of the inner core and the mass centre of the earth.

For a geophysical application, we have computed the degree-one deformation induced by the present-day mantle-density heterogeneity derived by Ricard *et al.* (1993). This model uses plate-motion reconstructions under the assumption that subducted slabs sink vertically into the mantle. It assumes no density contrast at 670 km and a viscosity jump of about 40 (see Table 3a). In Fig. 9 we show the present-day degree-one spectral amplitude of the density versus the depth. Note that the amplitude increases with depth. Consequently, the most important contribution to the CMB topography will come from the density heterogeneities located in the lower mantle, that is those related to subduction that occurred some 60 Myr ago. The induced topographies and equipotentials at the surface, the 670 km depth discontinuity, the CMB and the ICB are shown in Figs 10 and 11, respectively . The amplitude and direction of the resulting translation in topography and in equipotential at each interface of the earth are given in Table 4.

Note that at the earth's surface we obtain a translation of about 100 m in a direction near to the N–S axis. The present observed topography (Balmino, Lambeck & Kaula 1973) gives normalized coefficients of the degree-one spherical harmonic expansion $a_{10}=639$ m, $a_{11}=591$ m and $b_{11}=409$ m. Our computed values are one order of magnitude smaller than the observed ones and consequently we can conclude that the mantle-density heterogeneity derived by Ricard *et al.* (1993) can reasonably contribute to the surface topography. This surface translation expresses the discrepancy between the figure centre and the mass centre of the Earth.

At the CMB, we obtain a translation of about 870 m in the direction 151°, 19.7°, whereas at the ICB the translation of about 9 m is almost in the opposite direction (53.6°, −133°). The relative translation of each layer is carried out in order to conserve the centre of mass of the Earth. The amplitude of the degree-one topography at the CMB seems to be large in comparison with that obtained by seismological studies (e.g. Forte, Mitrovica & Woodward 1995), which is about 300 m. This point is also valid for higher degrees. We have seen that the density heterogeneity located in the bottom of the lower mantle contributes in a very important way to the CMB topography and it raises the problem of slabs sinking until they reach the CMB. The distance between the geometric centre of the homogeneous inner core (that is the centre of the initial reference sphere) and the mass centre of the earth induced by these mantle density heterogeneities is thus about 9 m in the direction 53.6°, −133°.

In Figs 12 and 13 we show the total deformation (topography and equipotential) at the CMB and the ICB induced by this mantle-density heterogeneity in the degree range 1 to 15 (from Greff-Lefftz & Legros 1996). Note that the CMB topography is larger beneath the Pacific belt, that is beneath the principal zones of subduction: in fact, the topography follows the density heterogeneities within the lower mantle very closely (see Fig. 4 of Greff-Lefftz & Legros 1996), which are related to subduction that occurred some 60 Myr ago, and thus are maximal over the Bering sea.

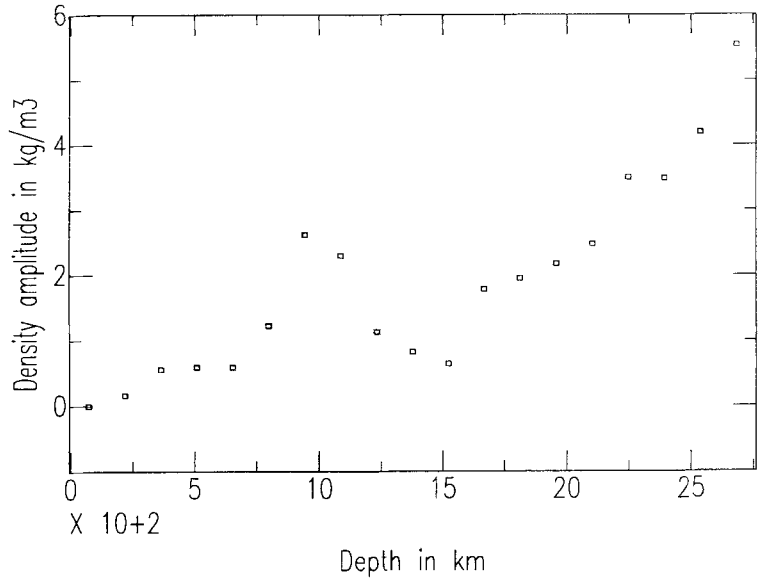

Figure 9. Degree-one spectral density of the mantle-density heterogeneity derived by Ricard *et al.* (1993) versus the depth. Note that the amplitude increases with depth.

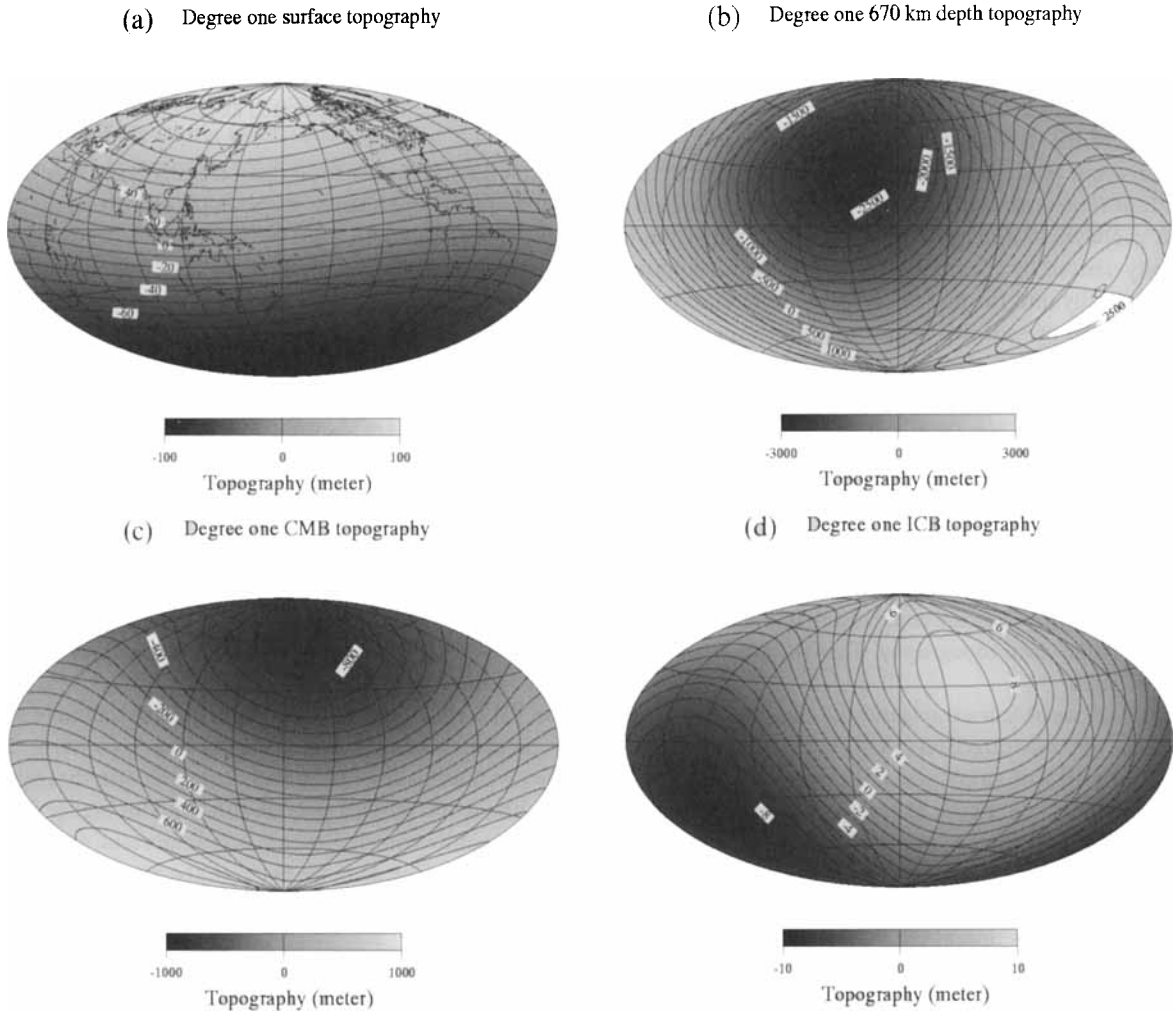

Figure 10. Degree-one radial displacement at the earth's surface (a) (contour interval 20 m), at the 670 km depth discontinuity (b) (contour interval 500 m), at the CMB (c) (contour interval 100 m) and at the ICB (d) (contour interval 1 m) induced by the mantle-density heterogeneity described in Fig. 9.

Table 4. (a) Degree-one normalized coefficients of the computed topography (at the surface, the 670 km interface, the CMB and the ICB) induced by mantle-density heterogeneity, and the amplitude and direction of the resulting translation. (b) Degree-one normalized coefficients of the computed equipotential (at the surface, the 670 km interface, the CMB and the ICB) induced by mantle-density heterogeneity, and amplitude and direction of the resulting translation.

(a) Topography Radius in km	a_{10} (in m)	a_{11} (in m)	b_{11} (in m)	Resulting translation (in m)	Direction (θ, φ) (in °)
6371	55.1051	−5.3610	6.3377	96.522	(8.56°, 130.2°)
5701	−820.5396	1127.5465	−763.4430	2753.63	(121.07°, −34.10°)
3480	−441.2536	228.6626	81.9422	872.421	(151.17°, 19.71°)
1225.5	3.0643	−2.8594	−3.0290	8.960	(53.66°, −133.35°)

(b) Equipotential Radius in km	a_{10} (in m)	a_{11} (in m)	b_{11} (in m)	Resulting translation (in m)	Direction (θ, φ) (in °)
6371	0.	0.	0.	0.	
5701	−13.8870	8.9475	−4.9303	29.8604	(143.66°, −28.85°)
3480	3.3356	−3.1123	−3.2965	9.7487	(53.66°, −133.35°)
1225.5	1.3784	−1.2862	−1.3621	4.0284	(53.66°, −133.35°)

Note that the equipotentials at the CMB and ICB are proportional: this is because the fluid core is outside the mantle mass anomaly and the potential at the CMB can be simply continued down to the ICB. The proportionality factor being $(c/b)^n$, the dominant terms in the ICB equipotential are the degree range 1 to 3. The ICB topography, with an order of magnitude of about

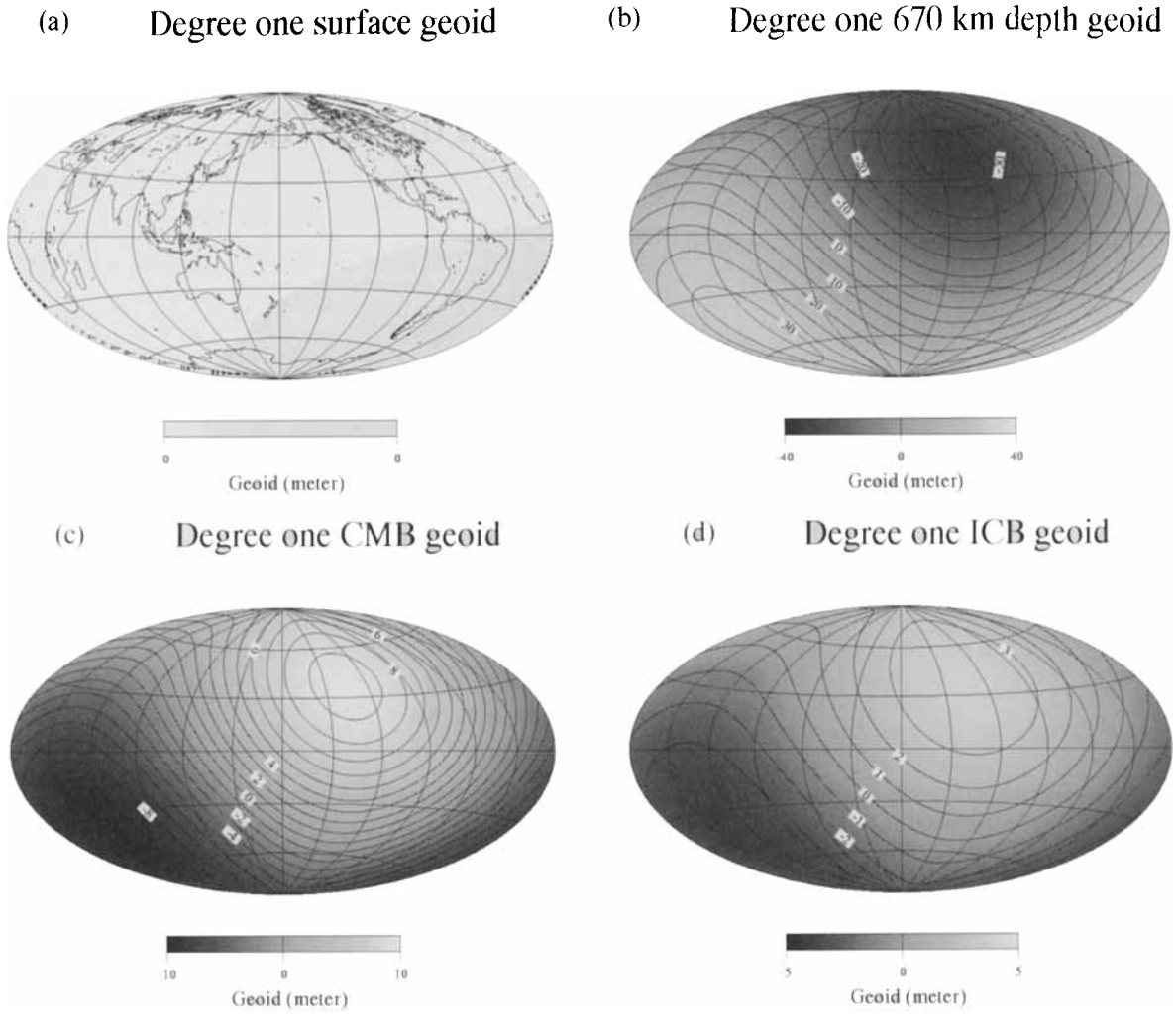

Figure 11. Degree-one equipotential at the Earth's surface topography (a), at the 670 km depth discontinuity (b) (contour interval 5 m), at the CMB (c) (contour interval 2 m) and at the ICB (d) (contour interval 0.5 m) induced by the mantle density heterogeneity described in Fig. 9.

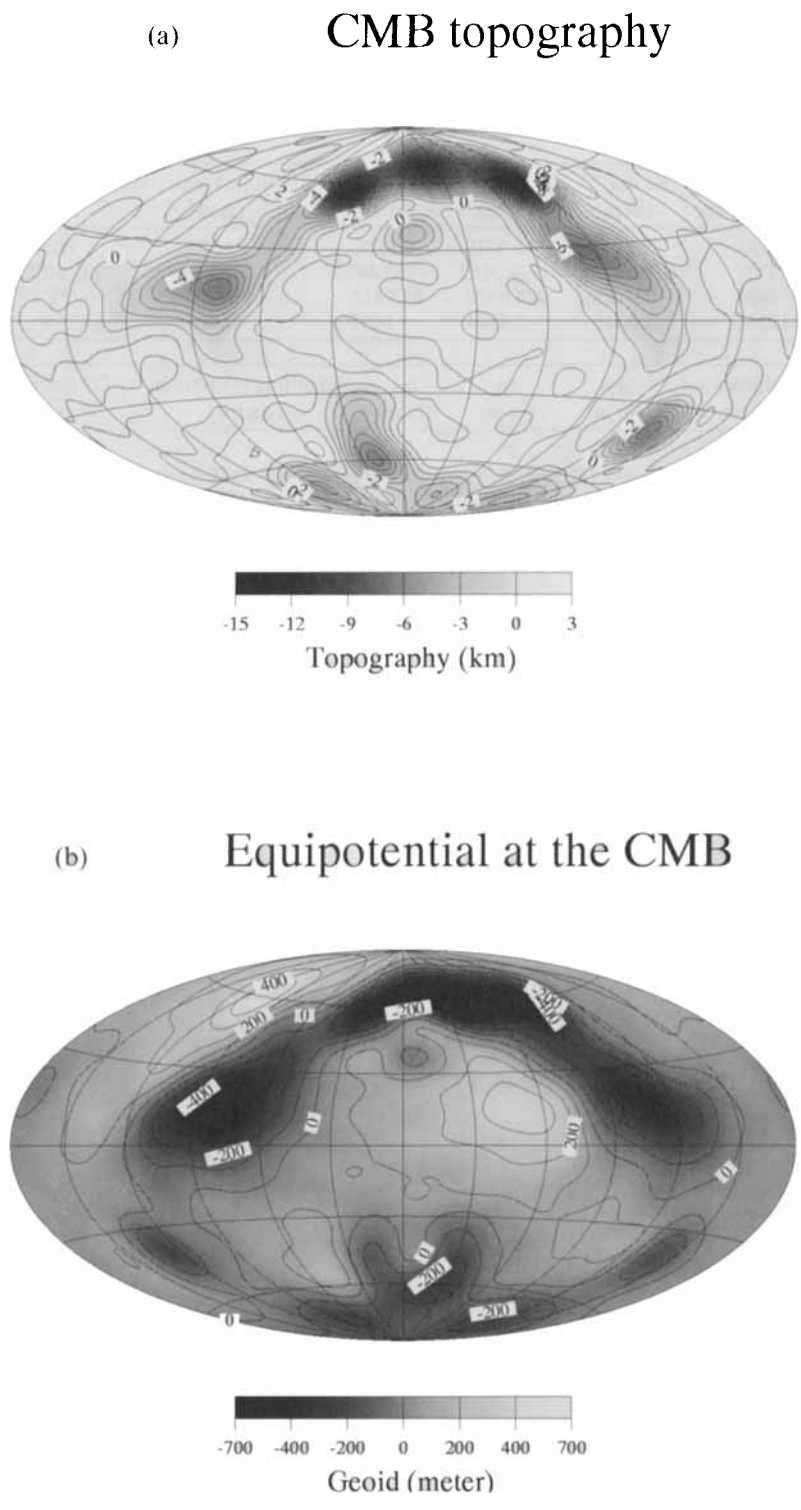

Figure 12. CMB topography (a) (contour interval 1 km) and equipotential (b) (contour interval 50 m) induced by the mantle-density heterogeneity of Ricard *et al.* (1993) in the degree range 1–15.

300 m, is exactly equal to

$$\frac{g(a)}{g(c)}\, y_5(c)\,,$$

that is the inner core is in hydrostatic equilibrium.

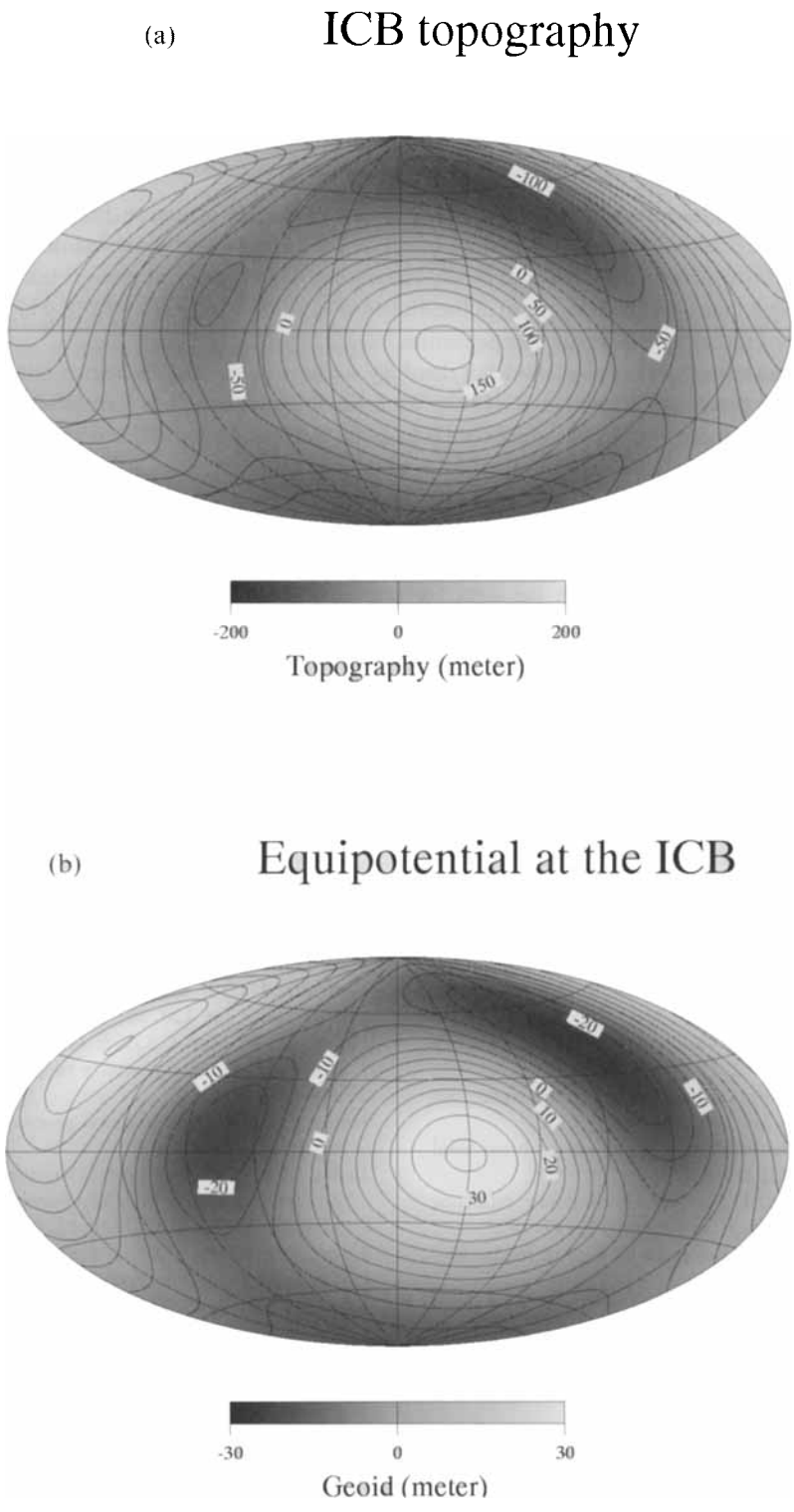

Figure 13. ICB topography (a) (contour interval 20 m) and equipotential (b) (contour interval 5 m) induced by the mantle-density heterogeneity of Ricard *et al.* (1993) in the degree range 1–15.

4 CONCLUSIONS

In this paper we have computed the degree-one elastic and viscoelastic deformation of an incompressible earth model. Our theoretical approach using a Love-number formalism has allowed us to do the following.

(1) Investigate the non-independent equations of the y_i system: we have shown that the last equation expresses the fact that the

total degree-one force acting on the Earth has to be equal to zero (Okubo & Endo 1986), which involves a relation between internal and external pressure and tangential traction.

(2) Using this approach, we have investigated the relaxation modes associated with the viscoelastic Love numbers induced by density, rigidity or a viscosity jump at the interfaces of our incompressible model: for degree one, the M_0 and G modes do not exist and a discontinuity in the Maxwell time involves only one transition mode (instead of two for degree $n \geq 2$).

As a geophysical application, we have computed the degree-one elastic deformation induced by atmospheric continental loading: we obtain, at each interface of the earth, translations of a few millimeters with a nearly annual period. At longer timescales, we have computed the viscoelastic deformation induced by the Pleistocene deglaciation: at present (almost 7000 yr after the end of the deglaciation), we find translations (of about a metre) in the direction $\theta_0 = 20.7°$ and $\lambda = -46.6°$E which tend to be relaxed, that is to be equal to zero, because of the surface isostatic compensation.

In a quasi-fluid approximation of the Maxwell model of rheology, we have computed the degree-one deformation induced by the mantle-density heterogeneities derived by Ricard *et al.* (1993). We have obtained a surface translation of the earth of about 100 m and a translation of the CMB of about 900 m. The inner core is in quasi-hydrostatic equilibrium and its centre of figure differs from the centre of mass of the earth by a distance of about 9 m.

ACKNOWLEDGMENTS

We thank Pascal Gegout for providing us with the data for continental loading and for his numerical computation of the degree-one loading Love numbers for a realistic earth model, and Y. Ricard for providing us with the data of the present-day mantle-density-heterogeneity model. This study was supported by a CNRS-INSU-DBT grant (contribution number 86).

REFERENCES

Alterman, Z., Jarosch, H. & Pekeris, C.H., 1959. Oscillation of the Earth, *Proc. R. Soc. Lond,* A, **252,** 80–95.

Balmino, G., Lambeck, K. & Kaula, W.M., 1973. A spherical harmonic analysis of the Earth's topography, *J. geophys. Res.*, **78,** 478–481.

Cathles, L., 1975. *The Viscosity of the Earth's Mantle,* Princeton University Press, Princeton, NJ.

Chinnery, M.A., 1975. The static deformation of an Earth with a fluid core: a physical approach, *Geophys. J. R. astr. Soc.*, **42,** 461–475.

Crossley, D. & Gubbins D., 1975. Static deformation of the Earth's liquid core, *Geophys. Res. Lett.*, **2,** 1.

Dahlen, F. & Fels, S., 1978. A physical explanation of the static core paradox, *Geophys. J. R. astr. Soc.*, **55,** 317–332.

Dahlen, F.A., 1993. Effect of the Earth's ellipticity on the lunar tidal potential, *Geophys. J. Int,* **113,** 250–251.

Dziewonski, A.M. & Anderson, D.L., 1981. Preliminary reference earth model PREM, *Phys. Earth planet. Inter.*, **25,** 297–356.

Farrell, W.E., 1972. Deformation of the earth by surface loads, *Rev. Geophys. Space Phys.*, **10,** 761–797.

Forte, A., Dziewonski, A.M. & Woodward, R., 1993. Aspherical structure of the mantle, tectonic plate motions, nonhydrostatic geoid and topography of the core–mantle boundary, in *Dynamics of the Earth's Deep Interior and Earth Rotation,* Geophys. Monograph, **72,** IUGG Vol. 12, 135–166.

Forte, A.M., Mitrovica, J.X. & Woodward, R.L., 1995. Seismic-geodynamic determination of the origin of excess ellipticity of the core–mantle boundary, *Geophys. Res. Lett.*, **22,** 1013–1016.

Gegout, P., 1995. De la variabilité de la rotation de la Terre et du champ de gravité, conséquente aux dynamiques de l'Atmosphère et des Océans, *PhD thesis,* Strasbourg, France.

Gegout, P. & Legros, H., 1997. The response of non-global static ocean to continental atmospheric loading, *Geophys. J. Int.*, submitted.

Gire, C. & Le Mouel, J.L., 1989. Tangentially geostrophic flow at the core–mantle boundary compatible with the observed geomagnetic secular variation: the large-scale component of the flow, *Phys. Earth planet. Inter.*, **59,** 259–287.

Greff-Lefftz, M. & Legros, H., 1995. Core–mantle coupling and polar motion, *Phys. Earth planet. Inter.*, **91,** 273–283.

Greff-Lefftz, M. & Legros, H., 1996. Viscoelastic mantle density heterogeneity and core–mantle topography, *Geophys. J. Int,* **125,** 567–576.

Hager, B., 1984. Subducted slabs and the geoid; constraints on mantle rheology and flow, *J. geophys. Res.*, **89,** B7, 6003–6017.

Hager, B., Clayton, R., Richards, M., Comer, R. & Dziewonski, A.M., 1985. Lower mantle heterogeneity, dynamic topography, and the geoid, *Nature,* **313,** 541–545.

Han, D. & Wahr, J., 1995. The viscoelastic relaxation of a realistic stratified earth and a further analysis of postglacial rebound, *Geophys. J. Int,* **120,** 287–311.

Hulot, G., Le Mouel, J.L. & Jault, D., 1990. The flow at the core–mantle boundary. Symmetry properties, *J. Geomag. Geoelectr.*, **42,** 857–874.

Hulot, G., 1992. Observations géomagnétiques et géodynamo, *PhD thesis,* Paris, France.

Lefftz, M. & Legros, H., 1993. Variation of J_2 and internal loads, in *Dynamics of the Earth's Deep Interior and Earth Rotation,* Geophys. Monograph, **72,** IUGG Vol. 12, 45–49.

Love, A.E.H., 1911. *Some Problems of Geodynamics,* Cambridge Universiy Press, Cambridge.

Merriam, J.B., 1985. Toroidal Love numbers and transverse stress at the Earth's surface, *J. geophys. Res.*, **90,** B9, 7795–7802.

Mitrovica, J. & Peltier, W.R., 1993. The inference of mantle viscosity from an inversion of the Fennoscandian relaxation spectrum, *Geophys. J. Int.*, **114,** 45–62.

Mitrovica, J.X. & Davis, J.L., 1995. Some comments on the 3-D impulse response of a Maxwell viscoelastic Earth, *Geophys. J. Int,* **120,** 227–234.

Mitrovica, J.X., Davis, J.L. & Shapiro, I.I., 1994a. A spectral formalism for computing three-dimensional deformations due to surface loads. 1. Theory, *J. geophys. Res.*, **99,** 7057–7074.

Mitrovica, J.X., Davis, J.L. & Shapiro, I.I., 1994b. A spectral formalism for computing three-dimensional deformations due to surface loads. 2. Glacial isostatic adjustment, *J. geophys. Res.*, **99,** 7075–7101.

Munk, W.H. & MacDonald, G.J.F., 1960. *The Rotation of the Earth,* Cambridge University Press, London.

Okubo, S. & Endo, T., 1986. Static spheroidal deformation of degree I. Consistency relation, stress solution and partials, *Geophys. J. R. astr. Soc.*, **86,** 91–102.

Peltier, W.R., 1974. Impulse response of a Maxwell earth, *Rev. Geophys. Space Physics,* **12,** 649–669.

Peltier, W.R. & Wu, P., 1983. Continental lithospheric thickness and deglaciation induced true polar wander, *Geophys. Res. lett.,* **10,** 181–184.Peltier, W.R., Drummond, R.A. & Tushingham, A.M., 1986. Post-glacial rebound and transient lower mantle rheology, *Geophys. J. R. astr. Soc.,* **87,** 79–116.

Ricard, Y., Richards, M., Lithgow-Bertelloni, C. & Le Stunff, Y., 1993. A geodynamical model of mantle density heterogeneity, *J. geophys. Res.,* **98,** 21 895–21 909.

Richards, M. & Hager, B., 1984. Geoid anomalies in a dynamic earth, *J. geophys. Res.,* **89,** B7, 5987–6002.

Saito, M., 1974. Some problems of static deformation of the earth, *J. Phys. Earth,* **22,** 123–140.

Smylie, D.E. & Mansinha, L., 1971. The elasticity theory of dislocations in real Earth models and change in the rotation of the Earth, *Geophys. J. R. astr. Soc.,* **23,** 329.

Spada, G., Yuen, D.A., Sabadini, R., Morin, P. & Gasperini, P., 1990. A computed-aided, algebraic approach to the post-glacial rebound problem, *Mathematica J.,* **1,** 65–69.

Spada, G., Sabadini, R., Yuen, D.A. & Ricard, Y., 1992. Effects on post-glacial rebound from the hard rheology in the transition zone, *Geophys. J. Int.,* **109,** 683–700.

Vermeesen, B., Sabadini, R. & Spada, G., 1996. Analytical visco-elastic relaxation models, *Geophys. Res. Lett.,* **23,** 697–700.

Wilhelm, H., 1983. Earth's flattening effect on the tidal forcing field, *J. Geophys.*,**52,** 131–135.

Wu, P. & Peltier, 1982. Viscous gravitational relaxation, *Geophys. J. R. astr. Soc.,* **74,** 377–449.

Wu, P. & Peltier, 1984. Pleistocene deglaciation and the Earth's rotation: a new analysis, *Geophys. J. R. astr. Soc.,* **76,** 753–791.

Wu, P., 1990. Deformation of internal boundaries in a viscoelastic earth and topographic coupling between the mantle and core, *Geophys. J. Int.,* **101,** 213–231.

Yuen, D.A. & Peltier, W.R., 1983. Normal modes of the viscoelastic Earth, *Geophys. J. R. astr. Soc.,* **69,** 495–526.